THE JOURNAL OF CHEMICAL PHYSICS

VOLUME 13, NUMBER 1 JANUARY, 1945

Publication of Papers from the Inaugural Meeting of the Division of High-Polymer Physics of the American Physical Society

THE following four articles were presented at the inaugural meeting, on June 23–24 of the Division of High-Polymer Physics of the American Physical Society. Because of the WPB restrictions on the use of paper, the original plan to publish all the papers presented at this meeting in the November, 1944 issue of the *Journal of Applied Physics* was abandoned; and some of them appear in this journal. A complete list of the papers presented at the meeting, with the present publication schedule, is given below.

Publication Schedule of Papers from June 23–24 Meeting of Division of High-Polymer Physics

1. A. V. TOBOLSKY AND R. D. ANDREWS—"Systems Manifesting Superposed Elastic and Viscous Behavior"	January, J. Chem. Phys. **13**, 3 (1945).
2. W. O. BAKER—"Transition Phenomena in High Polymers"	Paper not now available.
3. T. ALFREY—"A Contribution to the Kinematic Theory of Rubber Elasticity" (Publication title "Molecular Theory of the Viscoelastic Behavior of an Amorphous Linear Polymer")	September, J. Chem. Phys. **12**, 374 (1944).
4. B. A. MROWCA, S. L. DART, AND E. GUTH—"Retraction and Stress Propagation in Natural and Synthetic Gum and Tread Stocks"	January, J. App. Phys. **16**, 8 (1945).
5. R. S. HAVENHILL, H. C. O'BRIEN, AND J. J. RANKIN—"Electrostatic Properties of Rubber and GR-S"	November, J. App. Phys. **15**, 731 (1944).
6. R. B. STAMBAUGH, M. ROHNER, AND S. D. GEHMAN—"Speed of Retraction of Rubber"	November, J. App. Phys. **15**, 740 (1944).
7. S. L. DART AND E. GUTH—"Rise of Temperature on Fast Stretching of Butyl Rubber"	January, J. Chem. Phys. **13**, 28 (1945).
8. H. M. SMALLWOOD—"Limiting Law of the Reinforcement of Rubber"	November, J. App. Phys. **15**, 758 (1944).
9. F. L. ROTH AND L. A. WOOD—"Some Relations Between Stress, Strain, and Temperature in a Pure-Gum Vulcanizate of GR-S Synthetic Rubber"	November, J. App. Phys. **15**, 749 (1944).
10. F. S. CONANT AND J. W. LISKA—"Some Low Temperature Properties of Elastomers"	November, J. App. Phys. **15**, 767 (1944).
11. H. E. GREENE AND D. L. LOUGHBOROUGH—"Some Physical Properties of Elastomers at Low Temperatures"	January, J. App. Phys. **16**, 3 (1945).
12. H. MARK, P. M. DOTY, AND B. H. ZIMM—"Molecular Weight and Molecular Weight Distribution of High Polymers by Light Scattering Measurements"	Paper not now available.
13. E. GUTH—"Theory of Filler Reinforcement"	January, J. App. Phys. **16**, 20 (1945).
14. R. S. SPENCER AND R. F. BOYER—"Factors Influencing the Brittle Point of High Polymers"	Paper not now available.
15. S. L. GERHARD—"Kinematic Errors in Bobbin Drives on Roving Frames"	January, J. App. Phys. **16**, 26 (1945).
16. H. J. PHILIPP AND C. M. CONRAD—"Control of Elongation in Highly Stretched Cotton Tire Cord"	January, J. App. Phys. **16**, 32 (1945).

17. W. J. Lyons—"The Influence of Velocity Gradient on the Relation Between Viscosity and Concentration in Cuprammonium Solutions of Cellulose"	January, J. Chem. Phys. **13**, 43 (1945).
18. S. E. Sheppard and P. T. Newsome—"Orientation of Hydrophile Xerogels in an Electric Field"	Part I published in June, J. Chem. Phys. **12**, 244 (1944). Part II, December, J. Chem. Phys. **12**, 513 (1944).
19. D. R. Morey and J. W. Tamblyn—"Determination of Molecular Weights of High Polymers by Solubility Methods"	Paper not now available.
20. M. L. Huggins—"Comparison of the Structures of Stretched Linear Polymers"	January, J. Chem. Phys. **13**, 37 (1945).
21. J. W. Tamblyn, R. L. Tichener, D. R. Morey, and R. H. Wagner—"Fractionation, Viscosity, and Osmotic Pressure Studies on Cellulose Esters"	Paper not now available.
22. G. A. Anslow—"Ultraviolet Spectra of Biologically Important Molecules"	January, J. App. Phys. **16**, 41 (1945).
23. D. R. Elliott and S. A. Lippmann—"The Thermodynamics of Rubber at Small Extensions"	January, J. App. Phys. **16**, 50 (1945).

THE JOURNAL OF CHEMICAL PHYSICS VOLUME 13, NUMBER 1 JANUARY, 1945

Systems Manifesting Superposed Elastic and Viscous Behavior*

A. V. TOBOLSKY AND R. D. ANDREWS
Frick Chemical Laboratory, Princeton University, Princeton, New Jersey

(Received October 25, 1944)

Actual substances exhibit a very complicated behavior under mechanical stresses which cannot be described by classical elasticity theory nor by the classical theory of the hydrodynamics of viscous fluids. A general molecular theory describing the behavior of matter under stress is discussed and related to previous investigations and to experimental observations. Particular attention is devoted to rubberlike substances for which the classical theories are definitely inadequate. Experimental results on relaxation and creep of rubbers are interpreted in terms of modern structural concepts. It is found that these substances exhibit three regions of stress-temperature-time dependence. At intermediate temperatures there exists a region of relative stability in which the statistical-thermodynamic theory of rubber elasticity is valid. At elevated temperatures relaxation and creep are caused by chemical changes involving the rupture and formation of primary valence bonds. These chemical changes, which are responsible for the aging of rubber, can be isolated and studied by appropriate experimental techniques. At low temperatures relaxation and creep are caused by the slipping of secondary interchain bonds which are breaking and reforming in times comparable to experimental times of measurement. Theories are advanced to explain the observed stress-temperature-time behavior of rubbers over the entire temperature range studied.

THE theory of the mechanical behavior of deformable substances is divided into three parts. First there is the geometrical problem of defining the state of strain in a body. This problem has been solved in terms of the strain tensor for the case of small deformations. Secondly, there is the dynamical problem of defining the state of stress in a body and of extending Newton's laws of motion to derive equations of motion and equilibrium for non-rigid matter. Finally, it is necessary to postulate relationships between the components of the strain tensor and the components of the stress tensor. It is this aspect alone which relates to the specific nature of the substance involved. The classical theory of elasticity, which in certain ranges of deformation, temperature, and frequency applies very closely to the mechanical behavior of crystalline solids, is characterized by the assumption of Hooke's law which states that there is a linear relation between the components of stress and the components of strain. The classical theory of hydrodynamics, which applies very closely to the mechanical behavior of simple liquids and gases, is characterized by the assumption of Newton's viscosity law, which states that there is a linear relation between stress and rate of strain.

However, a very wide class of substances exhibits mechanical behavior in which elastic and viscous behavior are clearly superposed. Many of these substances, including rubbers, fibers, plastics, leathers, glasses, muscle tissue, and wood, are of great commercial or biological interest because of their complex mechanical behavior. The classical physicists, including illustrious men such as Maxwell and Boltzmann, were not unaware of the importance and theoretical interest attached to substances exhibiting superposed elastic and viscous behavior, and a classical theory for these phenomena was formulated.

Nearly a century ago Maxwell postulated an equation for one type of superposed elastic-viscous behavior, namely, the relaxation of stress in substances held at constant deformation, which phenomenon is particularly noticeable in substances such as pitch. The so-called Maxwell relaxation equation is:

$$\frac{ds}{dt}=\frac{1}{G}\frac{df}{dt}+\frac{1}{\eta}f, \tag{1}$$

where ds/dt is the rate of strain, f is the stress, G an elastic modulus, and η a coefficient of vis-

* Presented on June 23, 1944 before the Inaugural Meeting of the Division of High-Polymer Physics of the American Physical Society at Rochester, New York.

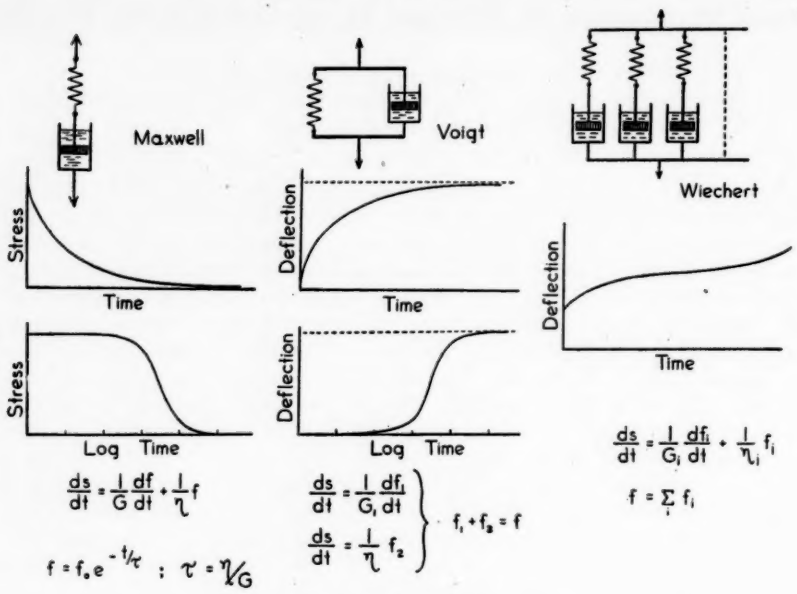

FIG. 1. Mechanical models of matter.

cosity. This equation corresponds to a mechanical model consisting of a spring and dashpot in series which we shall henceforth call a Maxwell element. If the strain is held constant ($ds/dt=0$) then the decay of stress at constant strain can be found by integrating Eq. (1) giving

$$f=f_0e^{-t/\tau}; \quad \tau=\eta/G, \tag{2}$$

where f_0 is the initial stress (at time $t=0$) and τ, the relaxation time, is defined as above.

The mechanical model corresponding to Maxwell's relaxation equation and graphs of the stress decay function plotted against linear and against logarithmic time are shown in Fig. 1.

The Maxwell theory is incomplete because it fails entirely to account for the phenomenon of creep under constant stress (or constant load). This behavior of matter can be readily paralleled by a mechanical model first introduced by Voigt, in which an elastic element (spring) and viscous element (dashpot) are placed in parallel. This, of course, corresponds to a linear differential equation for each element as shown in Fig. 1, the stress dividing itself in each member in such a way that the rate of strain is the same in each. In Fig. 1 are shown the differential equations corresponding to the Voigt model, and the deflection *vs.* time curves obtained from these equations. The Voigt theory is also incomplete because it does not account for relaxation of stress at constant elongation.

A theory that includes as special cases the results of the Maxwell and Voigt theories was proposed by Wiechert. The mechanical model suggested by Wiechert is simply a large number of Maxwell elements placed in parallel as shown in Fig. 1. Mathematically, this corresponds to a system of linear differential equations of the Maxwell type, the rate of strain appearing in each equation being the same throughout the system, and the partial stresses appearing in each equation each being an aliquot portion of the total stress. Each equation can be specified by a relaxation time, and in the general case an infinite number of Maxwell elements can be used by specifying a distribution of relaxation times.

It can be readily seen that this type of generalized theory can "explain" very complicated elastic-viscous behavior. However, the theory cannot be regarded as satisfactory without a sound molecular basis for interpreting the constants appearing in the equations in terms of the detailed structural theories of matter. Moreover, the assumptions concerning the linearity of the relations between stress and strain and stress and rate of strain need to be re-examined.

New interest in problems of general rheology

was awakened by the commercial development of synthetic rubbers, fibers, plastics, etc., whose physical properties could be controlled by various polymerization methods. This, together with new information and theories concerning the structure of polymeric materials, led to attempts to give specific meaning to the "springs" and "dashpots" of the classical theory in terms of the structural features of particular substances. Among the workers in this field were W. Kuhn, H. Mark, H. Leaderman, R. Simha, P. Kobeko, A. Lazurkin, J. D. Ferry, and many others. Simultaneously a deeper insight into the nature of molecular relaxation processes was achieved through the work of P. Debye, L. Prandtl, R. Becker, J. Frenkel, H. Eyring, R. Barrer, and other workers. Finally, in the field of rubberlike or high elasticity, a sound approach was provided by the work of H. Mark, K. H. Meyer, E. Guth, H. M. James, F. T. Wall, L. R. G. Treloar, and P. J. Flory.

It is impossible to detail the work of the various writers and workers in the field of elastic-viscous phenomena. Furthermore, inasmuch as the subject is still in a stage of rapid development, it is not possible to attain a proper perspective of the field as yet. For these reasons the following discussion will be restricted to work with which the authors have been directly connected: theoretical work of the senior author with Professor H. Eyring of Princeton University, and joint experimental-theoretical researches of both authors with Dr. J. H. Dillon and Mr. I. B. Prettyman of the Firestone Tire and Rubber Company, and Mr. R. B. Mesrobian and Mr. T. E. Allen of Princeton. The work of other authors is referred to only as it contributes directly to the single viewpoint adopted here.

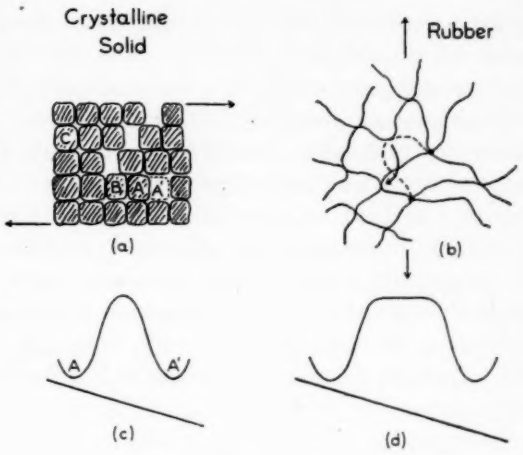

FIG. 2. Elastic-viscous processes.

ELASTIC-VISCOUS PROCESSES

The molecular processes that give rise to macroscopic elastic-viscous phenomena depend on the particular structural features of each new class of substances studied, but there are nevertheless certain underlying similarities in the ele-

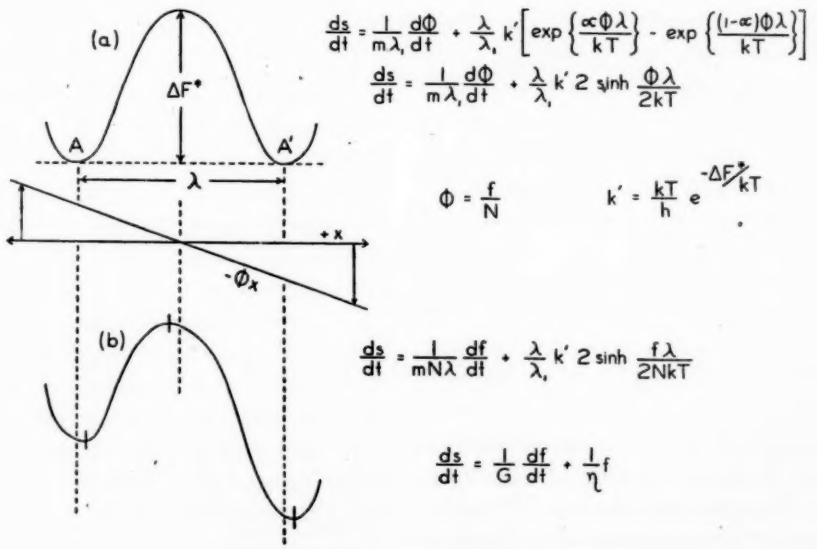

FIG. 3. Unit process of deformation.

mentary processes which are common to all condensed phases. It is necessary to idealize the situation and assume that in a body subjected to external stresses there exist certain regions of elementary molecular movements and readjustments to the stresses, that recur throughout the substance and are independent of the molecular movements in neighboring regions. We shall call the elementary process that occurs in such a region a "unit process of deformation," remembering that the motion of an atom, molecule, or group of atoms or molecules might be involved in this unit process. Figure 2 exemplifies the types of elastic-viscous processes that might occur in a crystalline solid and in substances such as rubber. Because of the external shearing stresses atom A in the crystal lattice might jump into the new position of equilibrium A', in addition to undergoing an immediate coherent change in the equilibrium distance to centers of neighboring atoms. It might also be that the unit process of deformation involves the two atoms A and B simultaneously moving to a new position of equilibrium. Not all unit deformation processes in the substance are alike. For example, in order for atom C, which is not near a defect, to jump to a new position of equilibrium, a large scale reorientation of neighboring atoms is necessary. Atom C will, however, move relative to other atoms because of the elastic shift of all lattice distances in the crystal under the action of the external shearing stress.

In Fig. 2 is also shown a typical unit process that occurs in polymeric networks such as rubber. Here too the external stress acts in two ways: It tends to uncoil elastically the portions of the molecular chains between network junctures, and at the same time it tends to cause a breaking and reforming in relaxed positions of the network junctures which are formed by secondary bonds between the chains.

For a quantitative formulation of the elastic-viscous behavior represented by a unit process of deformation, we imagine the atom or group of atoms involved in the unit process to be momentarily at rest and consider the free energy surface on which this atom or group of atoms moves. This free energy surface, shown in Fig. 2(c), arises, of course, from the interaction with neighboring atoms. At the instant under consideration the deformation unit is at equilibrium at point A and therefore occupies a minimum position in a free energy well. At point A' another position of equilibrium is available and therefore point A' corresponds to another minimum in the free energy surface. Between A and A' the deformation unit must move through energetically unfavorable configurations which correspond to a free energy hill. The effect of stress is to subtract a linear potential gradient from the original free energy configuration.

UNIT PROCESS OF DEFORMATION

Consider a molecule at equilibrium in a potential well at point A next to a new equilibrium position at point A' (see Fig. 3). The potential curve will for mathematical simplicity first be assumed to be of the form

$$\frac{\Delta F^{\ddagger}}{2}\left(1-\cos\frac{2\pi x}{\lambda}\right), \tag{3}$$

so that $\Delta F^{\ddagger}$ will be the free energy of activation for movement from one equilibrium position to the next and λ will be the distance between successive equilibrium positions. The coordinate x will be taken in the direction in which the local force owing to the field of external stresses is acting. The effect of this force is to add a linear term $-\phi x$ to the potential surface in which the molecule moves, where ϕ is the local force and x is the distance. The new potential surface after addition of the stress gradient is shown in Fig. 3(b).

The rate of deformation is given by the sum of two terms: In the first place, the unit at A will, under the action of stress, shift its position in the free energy well to a new position of equilibrium at B. This shift will occur in phase with the stress, and will be the elastic component of the deformation. The amount of elastic shift is related to the curvature of the free energy well.

Secondly, there will be a jumping over the barrier from A to A' as well as in the opposite direction. The free energy of activation in the forward direction will be less than that in the backward direction as shown in Fig. 3(b). The resulting net rate of flow in the forward direction will also contribute to the rate of shearing.[1]

[1] H. Eyring, J. Chem. Phys. **4**, 283 (1936).

In a previous publication[2] it was shown how the rate of strain resulting from the local force could be calculated exactly from the potential curve (3). The resulting expression is

$$\frac{ds}{dt}=\frac{\lambda^2}{2\pi^2\lambda_1\Delta F^{\ddagger}}\frac{d\phi}{dt}+\frac{\lambda^2 e^{-\Delta F^{\ddagger}/kT}}{\lambda_1 h}2\sinh\frac{\phi\lambda}{2kT}, \quad (4)$$

where ds/dt is the rate of strain, k is Boltzmann's constant, h is Planck's constant, and λ_1 is the root mean square distance between identical deformation units projected in a direction perpendicular to the plane over which the stress is considered.

For a more general free energy surface, which is, nevertheless, of the same general shape as shown in Fig. 3, the rate of strain is given by

$$\frac{ds}{dt}=\frac{1}{m\lambda_1}\frac{d\phi}{dt}+\frac{\lambda}{\lambda_1}k'2\sinh\frac{\phi\lambda}{2kT}, \quad (5)$$

where

$$k'=\frac{kT}{h}e^{-\Delta F^{\ddagger}/RT},$$

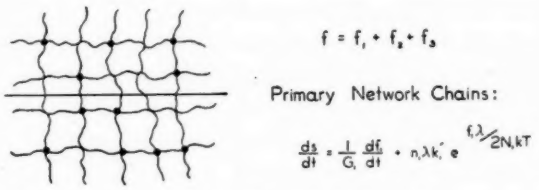

Secondary network chains (interchain forces):

$$\frac{ds}{dt}=\frac{1}{G_2}\frac{df_2}{dt}+n_2\lambda k_2'\,2\sinh\frac{f_2\lambda}{2N_2kT}.$$

Segment motion (intra-chain forces):

$$\frac{ds}{dt}=\frac{1}{G_3}\frac{df_3}{dt}+\frac{1}{\eta_3}f_3.$$

FIG. 4. Mechanical behavior of polymers.

where m is the curvature of the potential barrier near the minimum. It is to be observed that m is the force constant describing the interaction between molecules. It is clear that the first term on the right in Eq. (5) represents an elastic deformation, while the second term is a term representing flow.

In actual substances the structural features are such that we can classify together a number of unit processes of deformation, calling these processes of type i. Let there be ν_i such processes per unit volume. In general we shall wish to consider the effect of stress across a given plane of the medium. The direction perpendicular to this plane will be taken as the Z direction, and the total stress localized on the ith type of units will be called f_i.

Let the root mean square value of the projected distance along the Z axis between neighboring regions where processes of type i are occurring be λ_{1i}. Then it will be assumed that the local force on each process of type i is given by

$$\phi=\frac{f_i}{N_i}, \quad \text{where} \quad N_i=\nu_i\lambda_{1i}. \quad (6)$$

This assumption is valid if the total stress on each of the ith type of deformation units is distributed uniformly among these units.

Having established the very general rheological equations for the unit process of deformation, it remains necessary to specify the manner in which the external stress divides between various units, and how the macroscopic rate of strain relates to the rate of strain for the deformation units. For this the reasonable assumption is made that the medium retains the identity of its microscopic features under stress or deformation; in other words, it is assumed that the stress divides itself among the deformation units in such a way that the rate of strain is the same for each and equal to the macroscopic rate of strain. This is equivalent to the basic assumption of the Wiechert model. The general elastic-viscous equations from Eqs. (5) and (6) are

$$\frac{ds}{dt}=\frac{1}{m_i\lambda_{1i}}\frac{d\phi_i}{dt}+\frac{\lambda}{\lambda_1}k'2\sinh\frac{\phi_i\lambda_i}{2kT} \quad (7)$$

$$i=1, 2, 3\cdots,$$

where

$$\phi_i=f_i/N_i; \quad f=\sum_i f_i,$$

and

$$k'=\frac{kT}{h}e^{-\Delta F^{\ddagger}/RT}.$$

The symbols have been defined in the previous section; the subscript i refers to the ith type of unit process of deformation.

The theory presented here is therefore similar to the Maxwell-Wiechert theory. The chief differ-

[2] A. V. Tobolsky, R. E. Powell, and H. Eyring, *Frontiers of Chemistry: The Chemistry of Large Molecules* (Interscience Publishers, Inc., New York, 1943), Chapter V.

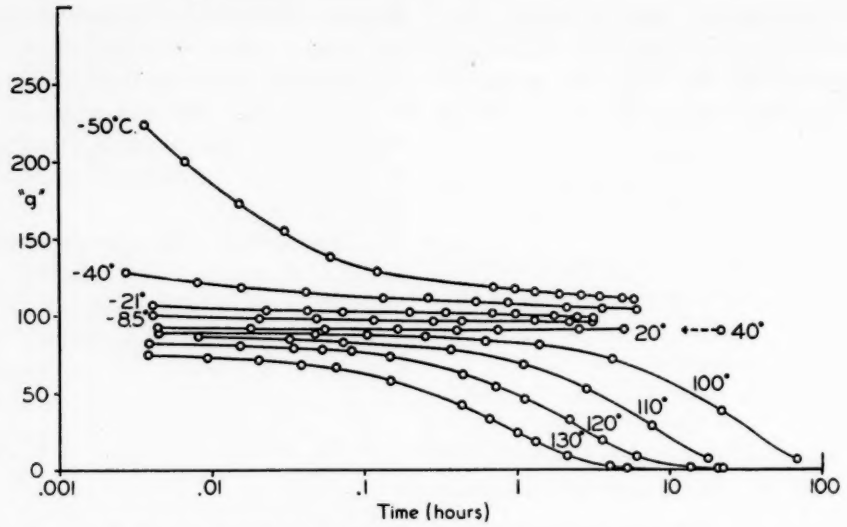

FIG. 5. "g" as a function of time for various temperatures; Hevea gum, 50 percent elongation.

ences lie in the fact that a non-linear flow term which becomes linear under the condition of small internal stress fields replaces the linear Newtonian flow term in Maxwell's equation, and the constants appearing in the equation are given specific molecular interpretation.

PHYSICAL PROPERTIES OF RUBBERLIKE MATERIALS

The general theory of superposed elastic-viscous behavior of matter presented in the previous sections must be supplemented by a detailed picture of the structural properties of the particular class of substances under consideration if useful application of the theory is to be made. In the remainder of this article we shall devote our discussion to polymeric materials in the rubbery state of aggregation—particularly natural and synthetic rubbers. These materials are characterized both by a long range and by a local structure. The long range structure is a polymeric network, the network junctures being composed of sparsely-occurring bonds between the coiled polymeric chains. These bonds may be primary cross links, or secondary interchain bonds such as dipole-dipole bonds or regions of local crystallinity. The portions of the network connecting contiguous network junctures are called network "chains." The local structure of the network is very similar to the local structure of liquids, the segments of the long chain molecules being in continual, fairly rapid motion, moving from one equilibrium position to the next. It is desirable to construct a theory of the over-all physical properties based on molecular quantities such as the number of network junctures of a given type per unit volume, the strength of these cross-linking bonds, and the internal viscosity of the local liquid-like structure.[3]

To find the relations between rate of strain, stress, and rate of stress over a given plane direction in a deformed rubberlike material we imagine a planar cut passing through the material in that plane. This cut will pass through a large number of network chains, some of which are terminated by primary cross links and others by secondary cross links. Let us denote by N_1 the number of chains (henceforth called primary network chains) terminated by primary cross links per unit area of the planar cut, and let N_2 denote the number of chains (henceforth called secondary network chains) terminated by secondary cross links per unit area of the planar cut. In general there may be more than one type of secondary cross link so that classifying all secondary network chains together is a simplification. If s_1 and s_2 are the number of primary and of secondary network chains per unit volume, respectively, then n_1 and n_2, where

$$n_1 = s_1/N_1; \quad n_2 = s_2/N_2,$$

[3] A. V. Tobolsky and H. Eyring, J. Chem. Phys. **11**, 125 (1943).

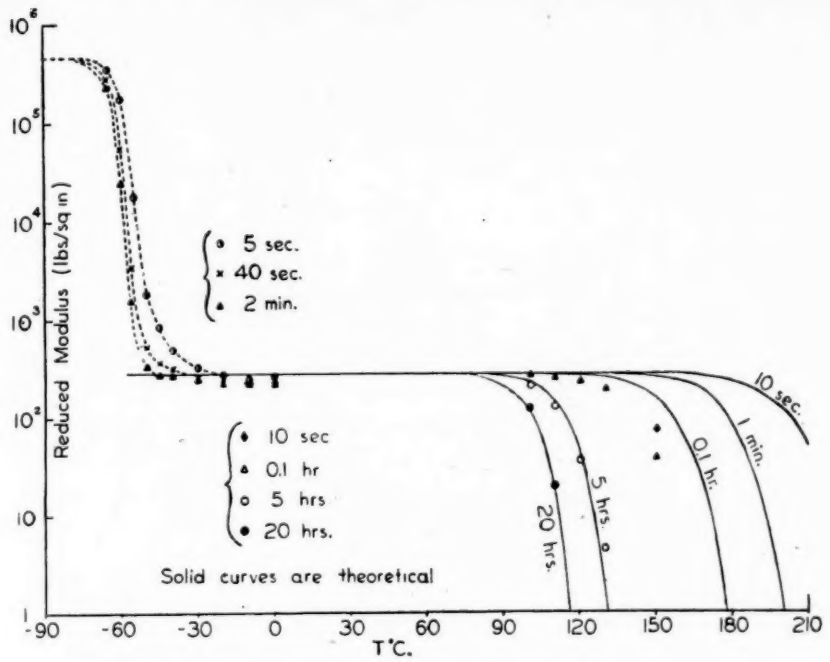

FIG. 6. Reduced modulus *vs.* temperature, Hevea gum.

are the reciprocal lengths between primary cross links and secondary cross links in the direction perpendicular to the planar cut.

The structural features described above are the deformation units in terms of which the elastic-viscous properties of these substances must be explained. The equations of motion for pure tension or pure shear for primary network chains and for secondary network chains in terms of the defined molecular quantities are shown in Fig. 4. The elastic term in these equations represents the uncoiling of network chains assuming that the terminal points (cross links) remain relatively fixed. The flow terms represent the contribution to the rate of deformation of rupturing processes at primary bonds along the chain which break the chains loose, and slipping processes occurring at the secondary cross bonds. The specific rate constants which appear in the equations of motion for primary network chains and for secondary network chains are defined by

$$k_1' = \frac{kT}{h} \exp\left(-\Delta F_1^{\ddagger}/RT\right);$$

$$k_2' = \frac{kT}{h} \exp\left(-\Delta F_2^{\ddagger}/RT\right);$$

where $\Delta F_1^{\ddagger}$ is the free energy of activation for the rupture of primary bonds, and $\Delta F_2^{\ddagger}$ is the free energy of activation for the breaking of secondary bonds. Generalization of these equations of motion to three-dimensional stresses and strains can be carried out readily.

A third type of unit process of deformation is included to account for the intra-chain motion of chain segments. These motions are such that the local environment of chain segments resembles the environment of molecules in the liquid state. This motion has a damping effect on the motion of the primary and secondary network chains as a whole, much as if a viscous liquid were pervading the network structure of the polymeric substance.

STATISTICAL THEORY OF ELASTICITY FOR RUBBER NETWORKS

The "high elasticity" of rubberlike substances is caused by the fact that under stress the "chains" between network junctures can uncoil.[4,5] In rubbers, for certain regions of temperature, the chains are very mobile, and as we shall see there

[4] F. T. Wall, J. Chem. Phys. **10**, 485 (1942).
[5] E. Guth and H. M. James, J. Chem. Phys. **11**, 455 (1943).

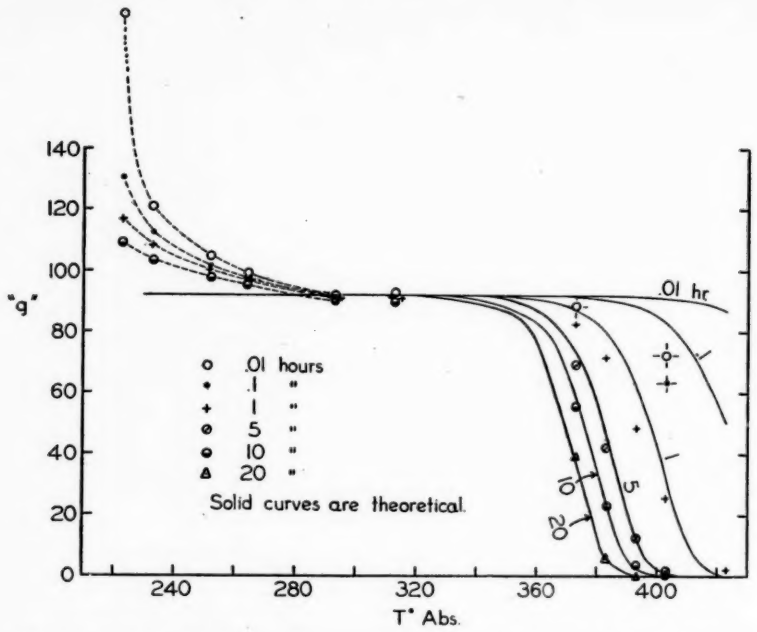

FIG. 7. "g" as a function of temperature for various times, Hevea gum.

is evidence that the internal energy of the network does not change as the network is stretched. The resistance to stretch is, therefore, caused by a decrease in entropy upon stretching, and this in turn is caused by the fact that the network chains can assume many more conformations in the unstretched state, where the distance between network junctures is small, than in the stretched state, where the distance between network junctures is larger.

From thermodynamics we can immediately derive the law

$$f=\left(\frac{\partial E}{\partial l}\right)_T-T\left(\frac{\partial S}{\partial l}\right)_T, \tag{8}$$

where f is tension, l represents length, E is internal energy, S is entropy, and T is temperature. Inasmuch as the first term on the right-hand side of Eq. (8) is taken equal to zero, the equation of state can be derived if we can relate S to l. This is done by relating S to the probability P by Boltzmann's relation

$$S-S_0=k \ln P/P_0, \tag{9}$$

where P/P_0 represents the ratio of the probabilities (or ratio of total number of available configurations) for the stretched and unstretched networks.

The evaluation of the probabilities P and P_0 is accomplished by determining the number of ways that a coiling hydrocarbon chain can assume a projected length x between its ends along any direction in space. The stable configuration for successive bond directions is believed to be the staggered configuration. The meanderings of a hydrocarbon chain can be described as a continuous path on a diamond lattice, each path being equally likely if we neglect the effect of steric hindrance.

Suppose that the total number of carbon-carbon bonds in the chain is n, and the bond length divided by $\sqrt{3}$ is taken as the unit of length. The problem of the random walk on a diamond lattice turns out to be equivalent to the problem of finding the distribution in heads of a penny that is being tossed n times and has a $\frac{2}{3}$ probability of repeating its last flip.

The result of a rather lengthy calculation[2] is that the probability of a chain of n bonds having the projected length x along any direction in space is

$$p_n(x)=\frac{1}{2\sqrt{\pi n}}\exp\left(-x^2/4n\right). \tag{10}$$

This formula can be directly applied to the the case where "ends" of the hydrocarbon chain

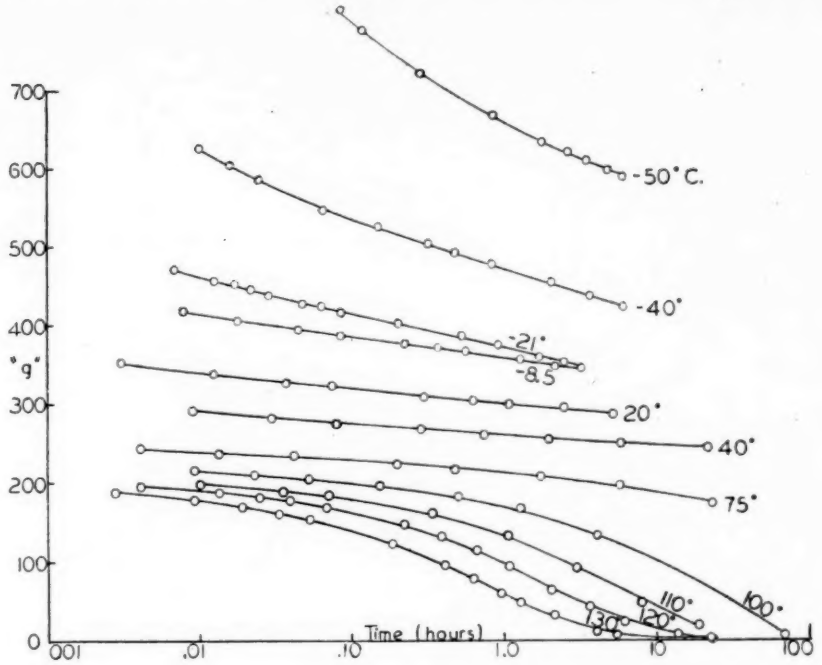

FIG. 8. "g" as a function of time for various temperatures, Hevea tread.

are successive juncture points in a polymer network. It is assumed that upon stretching there is a homogeneous change in the components of distance between successive network junctures throughout the rubber which is the same as the change in dimensions of the macroscopic sample. By averaging over all orientations and over all chains of the network, P/P_0 in Eq. (9) can be

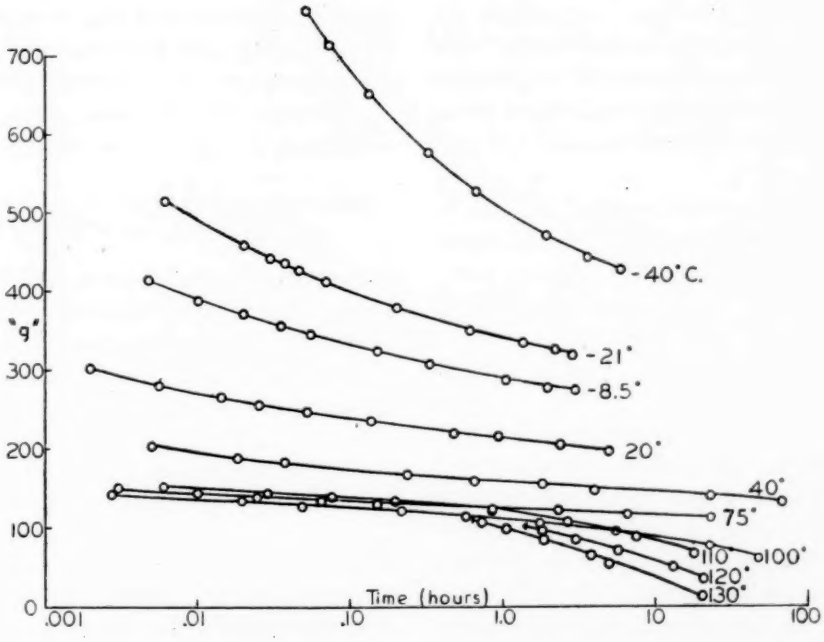

FIG. 9. "g" as a function of time for various temperatures, GR-S tread.

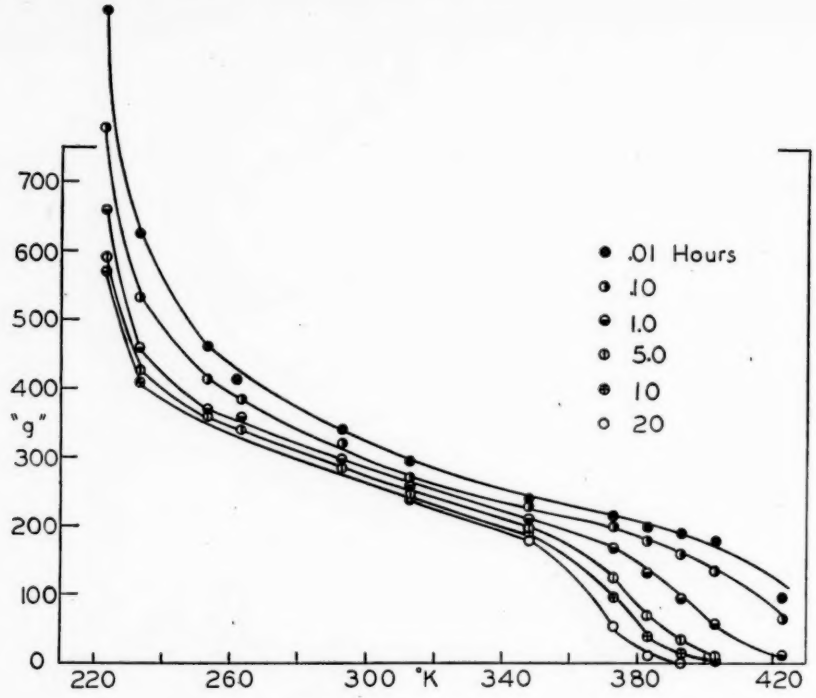

FIG. 10. "g" as a function of temperature for various times, Hevea tread.

evaluated, and thereby the stress-strain curve at equilibrium can be derived.[4,5] The result is:

$$f = skT\left\{\frac{l}{l_u} - \left(\frac{l_u}{l}\right)^2\right\}, \tag{11}$$

where l_u represents unstretched length, l the equilibrium length at tension f, and s represents the number of network chains of all kinds per cc that remain unbroken and unrelaxed at the time of measurement.

The values of the elastic moduli G_1 and G_2 appearing in the equations of Fig. 4 can be expressed as follows from Eq. (11):

$$G_1 = 3s_1kT, \tag{12}$$

$$G_2 = 3s_2kT, \tag{13}$$

where s_1 and s_2 are as defined above: the number of primary network chains per cc and the number of secondary network chains per cc, respectively. G_3 appearing in Fig. 4 is an ordinary elastic modulus for crystalline substances (the modulus in the case that the temperature is sufficiently low for segment motion to be completely frozen). Usually G_1 has a magnitude of about 10^6–10^7 dynes/cm^2 for soft rubber, whereas G_3 is of the order of magnitude of 10^{11} dynes/cm^2.

We have presented above a theory based upon *a priori* considerations concerning stress-strain relationships and upon several assumptions regarding the structural characteristics of rubber-like polymers. In the succeeding sections we shall show how experimental results bear upon this theory, and also how these results suggest modifications and extensions of the theory.

STRESS-TEMPERATURE-TIME RELATIONS FOR NATURAL AND SYNTHETIC RUBBERS

An equation has been given in the previous section which relates the stress and the elongation of a rubber sample in terms of the concentration of network chains in the rubber and the temperature, as follows:

$$f = skT\left\{\frac{l}{l_u} - \left(\frac{l_u}{l}\right)^2\right\}, \tag{14}$$

where f is the stress (calc. on original cross section), s is the number of network chains per cc of the rubber, k is Boltzmann's constant, T is the absolute temperature, l is the stretched

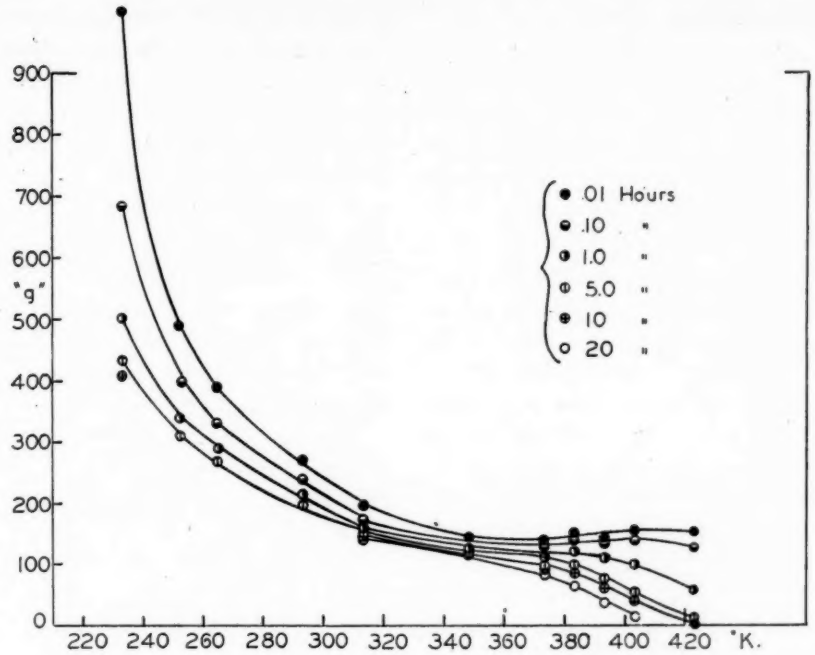

FIG. 11. "g" as a function of temperature for various times, GR-S tread.

length, and l_u is the unstretched length of the sample. Thus, according to this equation, any changes in the stress of a rubber sample held at constant temperature and constant elongation must be caused by changes in the number of network chains s per unit volume of the rubber that are effective in maintaining the stress. As can be seen from Eq. (14), changes in s can be measured in two ways: (1) one may keep the elongation l constant and measure the changes in f, or (2) one may keep f constant and measure the changes in l. The first method is referred to as "stress relaxation at constant elongation" and the second method as "tensile creep under constant load." Both types of measurement can be made in two different ways: First, one can keep the sample continuously elongated, or under load, as the case may be—this will be called the "continuous" method; or, one can elongate the sample or apply the load only momentarily when a measurement is taken, allowing the sample to remain unstretched at all other times—this will be called the "intermittent" method. Certain fundamental differences exist between the continuous and intermittent types of measurement, as will appear in the subsequent discussion.

Measurements of stress as a function of time in rubber samples held at constant elongation ("continuous relaxation"), using a variety of different rubber types, and made over a wide range of temperatures,[6] have indicated that for both natural and synthetic rubbers three general temperature regions can be distinguished: (1) a low temperature region of rapid change of stress with time, (2) an intermediate temperature region in which there is practically no change in stress with time, (3) a high temperature region in which there is again a marked decay of stress with time.

The low temperature region is the region in which stiffening of the rubber is observed because of the stability of secondary bonds (van der Waals bonds) between network chains. The relaxation of stress occurring in this region has been postulated as owing to the relaxing of these secondary bonds in the network structure (such as dipole-dipole bonds, etc.) which are partially stable during experimental times (roughly from 10 sec. to 10 hours) in that temperature range, and thus are able to contribute to the stress. The secondary bonds supposedly break and then reform in new, unstressed positions (where they no longer con-

[6] A. V. Tobolsky, I. B. Prettyman, and J. H. Dillon, J. App. Phys. **15**, 380 (1944).

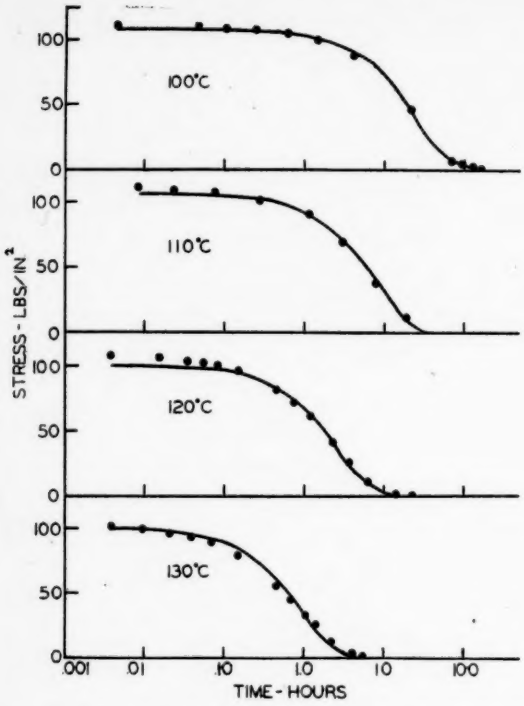

FIG. 12. Hevea gum stock; 50 percent elongation, theoretical curves, experimental points.

tribute to the stress) so that the changes occurring in the rubber during secondary bond relaxation are "reversible," and there is no permanent change in the rubber.

The high temperature region of instability of stress with time is that temperature region associated with "heat aging" phenomena—softening and hardening which permanently destroy the rubbery properties of the material. The relaxation of stress in this region is attributed to a definite chemical reaction which cuts chains by breaking primary valence bonds in the network structure; thus the changes in the rubber accompanying the relaxation of stress in this temperature region are not reversible, but cause a permanent deterioration of the network structure. This chemical scission reaction has been shown to require the presence of oxygen in order to occur, but only a slight amount of oxygen was found to be necessary.

In the intermediate temperature region secondary bonds are so unstable that they have all relaxed by the time the first stress reading can be taken, and the primary bond scission reaction is occurring so slowly that it produces no noticeable effect during the experimental time. It is in this intermediate temperature region of relative thermodynamic stability that statistical and kinetic treatments of rubber elasticity, which do not take time effects into account, have their greatest validity.

If experiments could be carried out at low enough temperatures, one might expect to find a fourth temperature region—a very low temperature region where secondary bonds as well as primary bonds would be completely stable within experimental times, and therefore there would be no change in stress with time.

The first three temperature regions mentioned above can be seen in Fig. 5, where continuous relaxation data for Hevea gum over the temperature range $-50°$ to $+130°$C are shown.* It will be noted that reduced stress, "g," has been plotted as the ordinate rather than the stress itself. The reason for this is that at a fixed elongation the stress is presumably proportional to the absolute temperature T as well as to the concentration of chains in the network s, as is seen from Eq. (14). Thus by eliminating the effect of temperature by "reducing" the stress values arbitrarily to 25°C (i.e., the stress f is multiplied by $298/T$ at each temperature T to give "g"), the stress values at different temperatures are then directly comparable in terms of s. There is considerable decay of stress observed in the low and high temperature data, whereas in an intermediate temperature range there is little change in stress with time. This is seen even more clearly in Fig. 6 where "reduced modulus" (modulus times $298/T$) at different fixed times is plotted against temperature. The ordinate could be changed to reduced stress simply by relabelling the ordinate scale (reduced modulus $= 2.985 \times$ reduced stress). The fact that the reduced modulus remains the same in this temperature range of stability means, of course, that the stress f is directly proportional to absolute temperature in this range. From this fact it can be proved thermodynamically that the assumption, made in all kinetic theories of rubber elasticity, that

* The data quoted here on relaxation of stress at constant extension are in general taken from reference 6 where complete details as to experimental procedure are given. In a few cases data which were obtained in connection with the experimental work on reference 6 but not published then are given here for completeness.

the internal energy does not change when the rubber is stretched, is correct. Consider the thermodynamic relation

$$\left(\frac{\partial E}{\partial l}\right)_T = -T\left(\frac{\partial f}{\partial T}\right)_l + f. \qquad (15)$$

If f is directly proportional to T, then by substituting in Eq. (15) obviously $(\partial E/\partial l)_T$ is equal to zero.

The experimental data in this graph were obtained from two sources: The data at 0°C and below were obtained from what might be considered a modified form of continuous creep experiment which measures modulus as a function of time. The experimental method, which has been described elsewhere,[7] measures the bending of a horizontal bar sample, supported at the ends and with a weight applied in the center, as a function of time. These modulus data are undoubtedly not completely comparable with continuous relaxation data, although the 5-sec. modulus points should correspond at least roughly to the 5-sec. stress relaxation values. The modulus data were used here because they extend down to −65°C, where the effect of secondary bonds becomes very important in Hevea gum, and the modulus data give some idea of the magnitude of the secondary bond effect.* Dotted curves have been drawn through the experimental points and extrapolated to a maximum flat value toward which the points seem to be converging. This flat would be expected to extend all the way down to 0°K. In this very low temperature region (−273°C to about −75°C) the effect of secondary bonds is so predominant that, if the flat value is approximately correct, less than a tenth of one percent of the stress is to be attributed to primary bonds in the network, all the rest being caused by secondary bonds. In this temperature region the rubber is essentially a crystalline solid, showing no rubbery properties whatever.

The high temperature experimental points were taken from the stress relaxation curves of Fig. 5. The solid curves drawn to accompany the high temperature data were calculated theoretically from Eq. (16), which will be discussed later. It is seen that they agree excellently with the 5-hr. and 20-hr. experimental points. Figure 7, which is replotted entirely from the data of Fig. 5, shows essentially the same points of interest as Fig. 6.

The thing particularly to be noticed in these graphs is the clear separation between the three (possibly four) temperature regions which have been discussed particularly the intermediate temperature region of stability of stress (or modulus) with time, which is clearly set off from the low and high temperature regions of instability, and which extends from about −10°C to +75°C.

In Figs. 8 and 9, stress relaxation data for

[7] J. W. Liska, Ind. Eng. Chem. **36**, 40 (1944).

* These data were kindly supplied us by Dr. J. W. Liska of the Firestone Physics Research Division, and have been more fully discussed by him at the June, 1944 meeting of the Division of High-Polymer Physics. We wish to thank Dr. Liska for extending this courtesy.

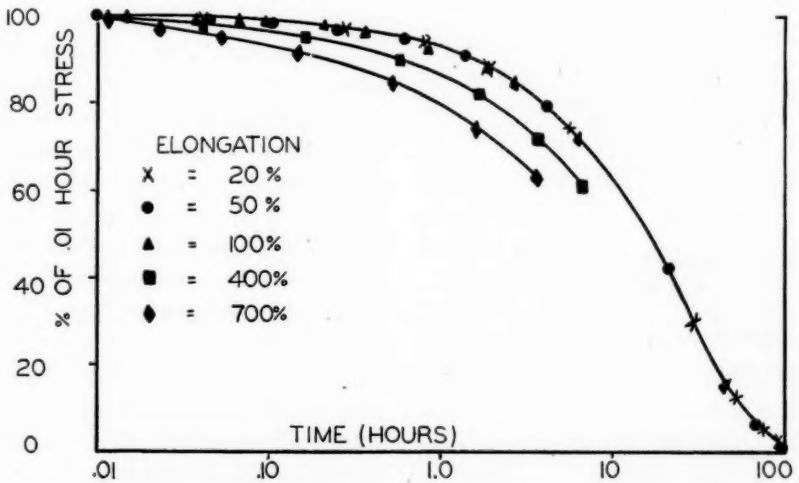

FIG. 13. Effect of percent elongation on relaxation rate; Hevea gum—100°C.

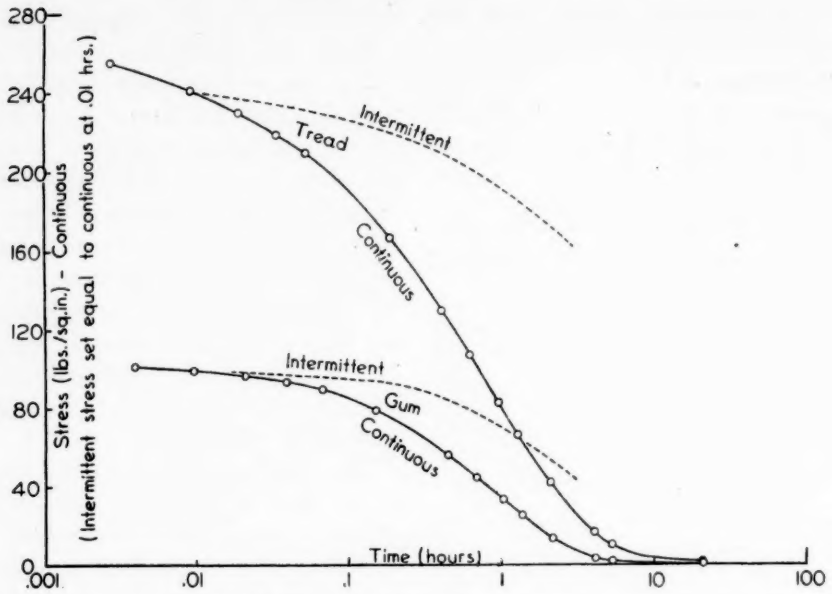

FIG. 14. Continuous and intermittent stress relaxation; 50 percent elongation; 130°C; Hevea stocks.

Hevea tread and GR-S tread are shown for the temperature range −50° to +130°C (the −50° curve for GR-S tread is not shown because the "g" values are too high to appear on the graph). In Figs. 10 and 11 the data from Figs. 8 and 9 are replotted as "g" *vs.* temperature at different fixed times. The most striking thing to be noticed in these latter graphs is that in these rubber stocks the secondary bond relaxation region overlaps the primary bond relaxation region to a much greater extent than is the case for Hevea gum. There is no temperature region in which the stress does not change with time. However, one can distinguish a roughly defined region where the stress does not change greatly with time. This is the general rule rather than the exception; Hevea gum is unique among those rubbers studied in its wide, clearly defined temperature region of stress stability.

HIGH TEMPERATURE PRIMARY BOND PHENOMENA

The high temperature stress relaxation curves of Hevea gum are found to fit the simple unimolecular rate law:

$$f=f_0e^{-k't}, \tag{16}$$

where k' is of course the rate constant of the process, f is the stress at time t, and f_0 is the initial stress. The dependence of the relaxation rate on temperature is given by the equation

$$k'=\frac{kT}{h}e^{-\Delta F^{\ddagger}/RT}=\frac{kT}{h}e^{-\Delta H^{\ddagger}/RT}e^{\Delta S^{\ddagger}/R}, \tag{17}$$

where k is Boltzmann's constant, T is absolute temperature, h is Planck's constant, R is the gas constant, $\Delta F^{\ddagger}$ is the free energy of activation, and $\Delta H^{\ddagger}$ and $\Delta S^{\ddagger}$ the heat and entropy of activation, respectively. It is found in fitting the experimental curves of Hevea gum that $\Delta F^{\ddagger}=30.4$ kcal., and that the free energy of activation is entirely heat of activation, $\Delta S^{\ddagger}$ being equal to zero. The success with which the experimental data can be fitted with Eqs. (16) and (17), taking $\Delta F^{\ddagger}$ equal to 30.4 kcal., is seen in Fig. 12, where experimental points and calculated curves are shown for Hevea gum at 100°, 110°, 120°, and 130°C.

Of all the various natural and synthetic rubbers studied, Hevea gum is the only rubber whose relaxation of stress curve follows the simple unimolecular decay law (16). Nevertheless, if the "relaxation rate constant" k' of these other rubbers at any temperature is taken as the reciprocal of the time at which $f/f_0=e^{-1}=1/e$ [as is properly true only of rubbers obeying

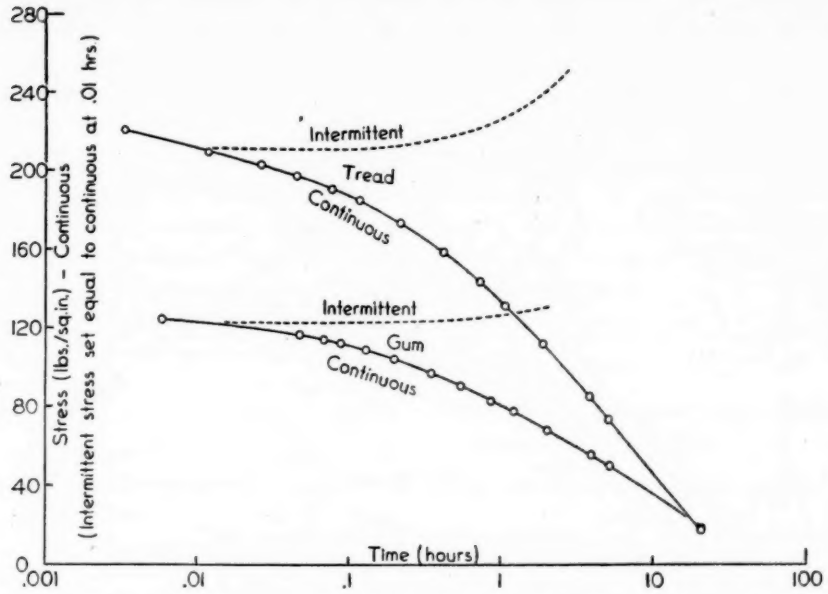

FIG. 15. Continuous and intermittent stress relaxation; 50 percent elongation; 130°C; GR-S stocks.

Eq. (16)], it is found that the temperature dependence of the "rate" is given by Eq. (17), just as for Hevea gum. The values of $\Delta F^{\ddagger}$ obtained for these various rubbers all fall within the range 30.4 ± 2.0 kcal., with $\Delta S^{\ddagger}$ again equal to zero; and although these differences correspond to large practical differences in relaxation rates, the fact that $\Delta F^{\ddagger}$ is about the same in all cases suggests that the mechanism of relaxation is of the same type in all. As mentioned before, this high temperature relaxation mechanism has been shown to be a scission process occurring in the presence of oxygen. By carrying out the relaxation experiments in purified nitrogen (highly oxygen-free), the relaxation rates of both natural and synthetic rubbers could be reduced about 1000-fold. Also, in a continuous creep experiment on a natural rubber stock, carried out at 110°C in a vacuum of 10^{-5} mm of Hg, the creep rate was perhaps a thousand times less than that observed in air at the same temperature.

The effect of elongation on the relaxation rate is illustrated for Hevea gum in Fig. 13. It is seen that in the range of 20 percent to 100 percent elongation, the relaxation curves obtained are identical (the five curves have been set equal at 0.01 hr. to facilitate comparison), showing that elongation has no effect in this range. However, at 400 percent and 700 percent elongation, the rate of relaxation is seen to be increased, most so at 700 percent. A possible explanation for this is that at these very high elongations some of the molecular chains may have uncoiled to their maximum possible extent, and the valence angles of the carbon atoms in the chains are being strained, which makes it easier to break the chains.

The general shape of the relaxation curve is characteristic of the rubber being used. The curves of the other rubbers are in every case more spread out in a log time plot than the unimolecular relaxation curve of Hevea. By comparing the relaxation curves of various gum stocks with the curves of the corresponding tread stocks, one finds that the presence of carbon black in the vulcanizate has comparatively little effect on the relaxation rate. The main effect of the carbon black is to increase the magnitude of the stress (see Figs. 14 and 15). The relaxation rate can be definitely slowed down, however, by the addition of antioxidant to the vulcanizate, the difference in rates being perhaps a factor of three or four. On the other hand, changing from sulphur to non-sulphur cures does not markedly affect the relaxation curves.

After this brief discussion of the main characteristics of relaxation curves obtained by the "continuous" method (constant elongation), we

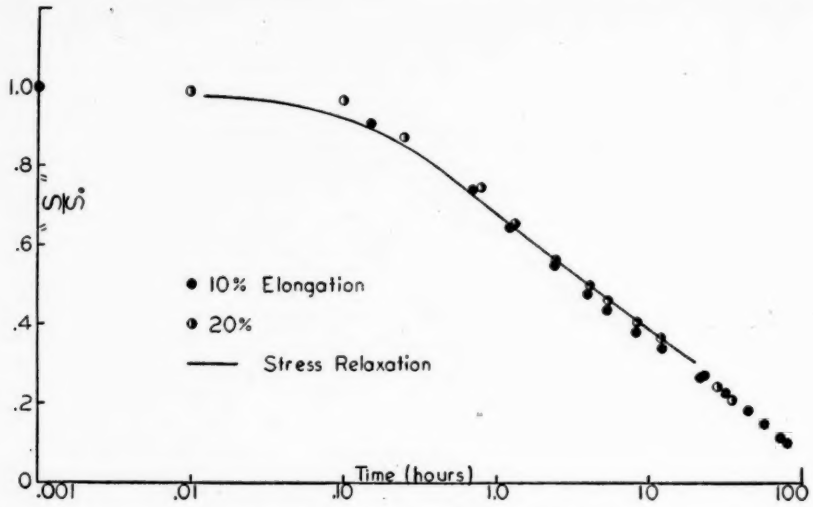

FIG. 16. Continuous creep; Butyl gum 120°C.

now turn to a consideration of "intermittent" relaxation curves. These intermittent stress relaxation measurements are really simply periodic measurements of the modulus of the sample, and the curve obtained could be called a "modulus *vs.* time" curve instead of an "intermittent stress relaxation" curve if one so desired. The thing immediately noticed in examining the intermittent relaxation curves is that the intermittent curve differs markedly from the continuous curve of the same rubber (see Figs. 14 and 15). In the continuous relaxation curves the stress always decreases continuously, and eventually reaches zero if the experiment is carried out for a long enough time. In the intermittent curves a remarkable variety of behavior is observed: The stress may decrease regularly, or increase regularly from the beginning; the stress may remain practically constant for a time, then begin to increase, or decrease; and in one case (Hevea at 100°C) the stress was observed to decrease initially, reach a minimum, and then increase. It is observed, in comparing the continuous and intermittent relaxation curves of any rubber, that the stress values of the intermittent curve are always greater than the stress values of the continuous curve; even when the continuous stress has decayed to zero, there is usually a sizable stress at that time in the intermittent curve. This accords with the observation that in those rubbers whose intermittent curve increases with time, when the stress has decayed to zero in a sample held at constant elongation, the sample is actually found to be very hard, with an extremely large modulus. This might seem rather surprising, since from Eq. (14) one would expect that when the stress had decayed to zero, there would be no network chains s left in the rubber, and the rubber sample would be very soft with no elasticity remaining. An increase or decrease of stress in the intermittent curve corresponds to the hardening or softening which one observes in examining the rubber sample, since the experiment is simply a periodic measurement of the modulus.

Apparently the explanation of these various observations is that at high temperatures *two* reactions are occurring simultaneously in the rubber: one a scission or breaking of molecular chains, and the other a cross linking of chains. The two reactions are competing with each other, and the intermittent curve measures the *net* change in the number of network chains per cc of the rubber, resulting from the combined effect of both reactions. But apparently the new network chains formed by cross linking are always formed in relaxed, equilibrium configurations, so that their formation does not increase the stress of a sample being held at constant elongation. For this reason the continuous relaxation curve is completely unaffected by the cross-linking reaction, measuring only the cutting of those network chains supporting the stress (i.e., those chains originally present in the rubber). Thus

the continuous relaxation curve isolates the scission reaction, while the intermittent relaxation curve measures the net effect of both reactions. The intermittent relaxation curve indicates whether scission or cross linking is predominating in the rubber. The intermittent stress values constantly increase in GR-S, which indicates that cross linking predominates over scission in GR-S from the beginning. The intermittent curve of Butyl decreases rapidly after a period of slight decrease, indicating that scission predominates in Butyl. In Hevea the intermittent curve first decreases, then increases, which indicates that scission predominates initially, but is eventually overtaken by cross linking. These trends correspond exactly to the observations that GR-S hardens, Butyl softens, and Hevea first softens, then hardens in heat aging.

Continuous and intermittent creep measurements made at high temperatures are also to be interpreted in terms of the scission and cross linking of the rubber molecules.[8] Intermittent creep measurements are, like intermittent relaxation measurements, simply a periodic measurement of the modulus of the sample, made in an alternate way. Both intermittent creep and intermittent relaxation data give the same curve when they are plotted in an equivalent way, and, of course, measure the same quantity—the net result of cross linking and scission. The most satisfactory way to plot relaxation and creep data in an equivalent way is to plot s/s_0 as the ordinate for both—the number of chains per cc of the rubber at time t divided by the number of chains per cc at zero time. Both types of data can be cast into this form by use of Eq. (14). At zero time we may write that

$$f_0 = s_0 kT\left\{\frac{l_0}{l_u} - \left(\frac{l_u}{l_0}\right)^2\right\}, \tag{18}$$

where the zero subscripts indicate zero time. Correspondingly at time t:

$$f = skT\left\{\frac{l}{l_u} - \left(\frac{l_u}{l}\right)^2\right\}. \tag{19}$$

To obtain s/s_0 we now divide (19) by (18), transpose all but s/s_0 to the other side, and cancel where possible. For stress relaxation, both continuous and intermittent, $l = l_0$ and so we obtain the simple expression

$$s/s_0 = f/f_0. \tag{20}$$

The significance of s is not the same in the two cases, however: In the intermittent data s signifies the total number of network chains per cc of the rubber at time t; in the continuous data s is the number (per cc) of those network chains present in the rubber at zero time which still remain uncut at time t. The significance of s_0

[8] R. B. Mesrobian, R. D. Andrews, and A. V. Tobolsky, incorporated in Senior Thesis of Mr. R. B. Mesrobian, Princeton University (1944).

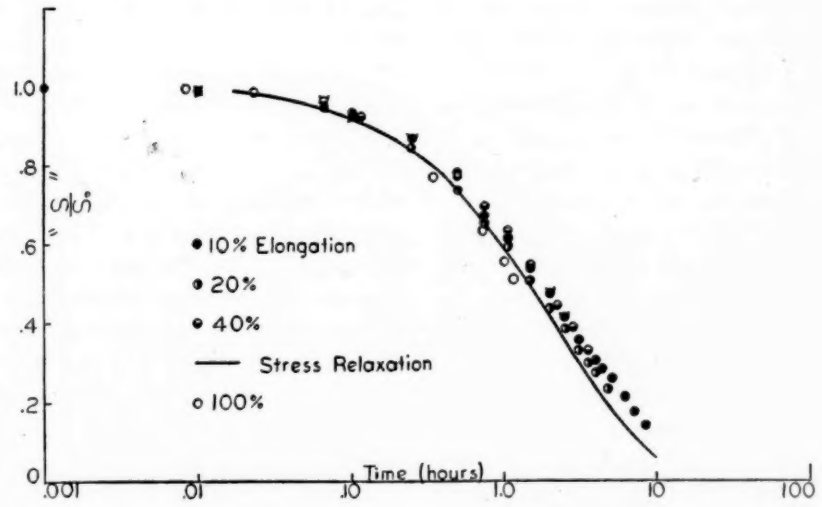

FIG. 17. Continuous creep; Hevea gum 120°C.

is the same for both: The total number of network chains per cc of the rubber at zero time.

For "creep under constant load," both continuous and intermittent, remembering that $f=f_0$, we obtain from Eqs. (18) and (19) the expression

$$s/s_0=\left\{\frac{l_0}{l_u}-\left(\frac{l_u}{l_0}\right)^2\right\}\Big/\left\{\frac{l}{l_u}-\left(\frac{l_u}{l}\right)^2\right\}. \quad (21)$$

Here s/s_0 for intermittent creep has the same significance as for intermittent relaxation. In continuous creep, however, a complication enters. If only scission were taking place in the rubber the continuous creep curve would be identical with the continuous relaxation curve (in fact, all four types of curve would be identical). But cross linking is always taking place at the same time; and although the new chains are in unstressed, equilibrium configurations at the moment of formation, the elongation of the rubber is constantly increasing, and as soon as the elongation becomes greater than that at which any chain was formed, that chain begins to help support the load. The contribution of these new chains to the stress, however, is not as great as that of the chains originally present in the rubber; this is because the l_u of these chains is the elongation of the sample at which they were formed rather than the original unstretched length of the sample, and l/l_u for these chains at any particular l is therefore less than the l/l_u for the original chains. Thus the cross linking has a retarding effect on the creep rate, and from the considerations given above we would expect the continuous creep curve to be slightly slower than the continuous relaxation curve, the divergence being greatest in those rubbers in which the cross-linking reaction is most marked. This is found experimentally to be the case. Continuous creep data for Butyl, Hevea, and GR-S are shown in Figs. 16 to 20. Since the continuous creep curve measures principally scission, but does reflect to some extent the cross linking going on at the same time, the ordinate is labelled "s/s_0," the quotation marks indicating that the continuous creep values are only pseudo values of the true s/s_0 as measured by continuous relaxation. The corresponding continuous relaxation curves are shown as solid lines. Continuous creep data at more than one initial elongation are generally shown, incidentally illustrating that the creep curves obtained are identical, within experimental error, from 20 percent to 100 percent initial elongation.

It will be seen that no noticeable deviation from the stress relaxation curve is observed in the continuous creep data of Butyl gum at 120°C (Fig. 16). The creep data of Hevea gum at 120°C are slightly slower than the relaxation curve (Fig. 17), but not to any great extent. In both of these rubbers scission is predominant (in the experimental time the rate of cross

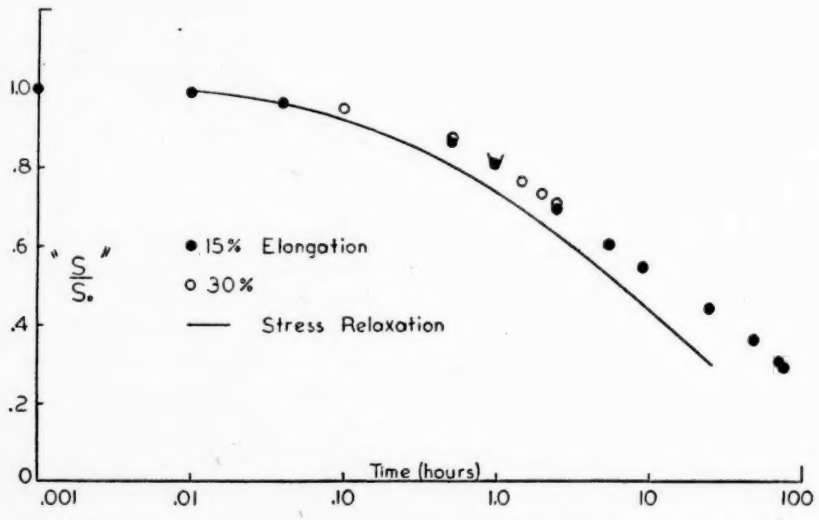

FIG. 18. Continuous creep; GR-S gum 120°C.

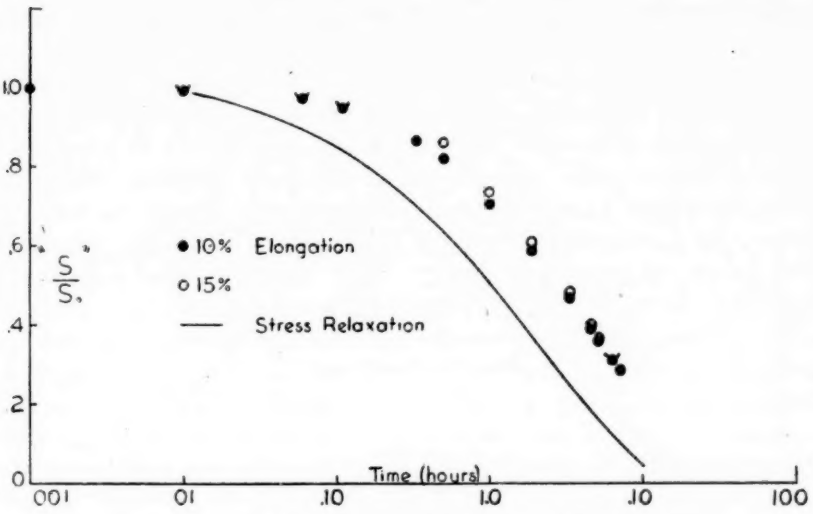

FIG. 19. Continuous creep Hevea tread 120°C.

linking has not overtaken the rate of scission in Hevea gum). In Fig. 18 continuous creep data at 120°C are shown for GR-S gum, in which cross linking predominates over scission, and which would therefore be expected to show a more marked effect. It is seen that the deviation of the creep data from the relaxation curve is significantly greater in GR-S gum than in Butyl and Hevea gums.

The effect of carbon black can be seen by comparing Hevea tread and GR-S tread (Figs. 19 and 20) with the corresponding gum stocks (Figs. 17 and 18). It is seen that the deviation is greater in the tread stock than in the gum stock in both cases; this is observed to be the general case. This would seem to indicate that cross linking occurs more rapidly in the tread stock than in the gum stock, though the rate of the scission reaction has been found to be about the same in both. This is confirmed by a comparison of the continuous and intermittent relaxation curves of gum and tread stocks in Figs. 14 and 15. The explanation of this fact is not clear at the present time. It has been suggested that the rubber molecules cling to the surface of the carbon black particles in tread stocks, thereby giving the rubber a higher modulus. It may be that the carbon black particles bring the chain molecules closer together in this way, and thus make cross linking easier, the effect being the opposite of that of swelling agents, which will be discussed in the following section.

This high temperature oxidative scission and cross linking do not manifest themselves only in continuous and intermittent relaxation and creep measurements. Another interesting manifestation is in the dissolution of vulcanizates. When pieces of vulcanizate are heated at fairly high temperatures in a good swelling liquid (such as toluene or xylene), in the presence of small amounts of oxygen, the vulcanizate eventually disintegrates and goes into solution. This is true even of GR-S, in which cross linking occurs more rapidly than scission when the rubber is heated in air at the same temperatures. The explanation of this phenomenon apparently is that when the solvent swells the rubber, the molecular chains of the network are pushed farther apart, making cross linking more difficult, while molecular scission remains as easy as before. Thus in swollen GR-S vulcanizate, scission apparently takes place more rapidly than cross linking and eventually is effective in completely disintegrating the network of the polymer. The breaking of the network is caused not by the swelling force of the solvent, but by the effect of swelling in changing the relative rates of cross linking and scission in the polymer. When solvents which are not good swelling agents (i.e., water, acetic anhydride, castor oil) are used under the same conditions, dissolution does not occur, and the cross-linking reaction actually hardens the GR-S vulcanizate.[9] The

[9] Unpublished experiments of M. Magat and A. V. Tobolsky.

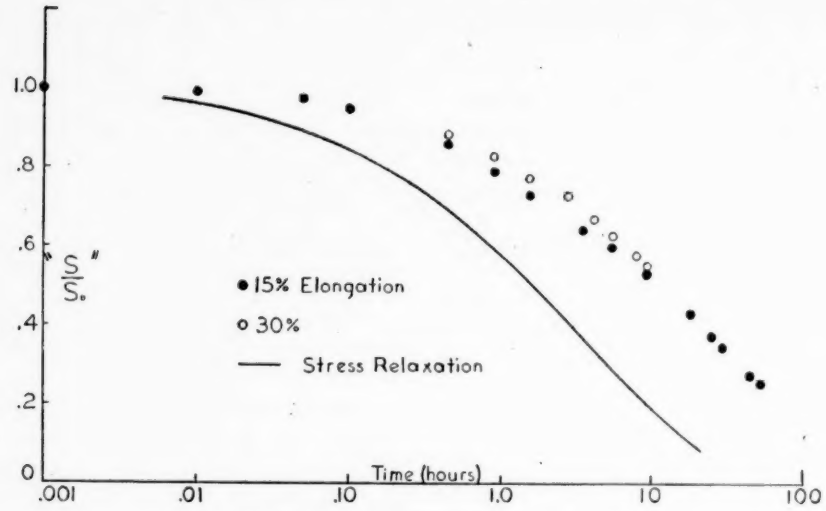

FIG. 20. Continuous creep GR-S tread 130°C.

time required for dissolution is roughly the time required to relax fairly completely in a continuous relaxation test.

The measurement of high temperature cross linking and scission in raw polymer must be done with special methods. Stress relaxation and creep can of course only be used with vulcanizates. One method of attack is provided by the fact that the molecules of raw polymer can be divided into two groups on the basis of their solubility in a good rubber solvent (benzene or toluene, for example). There is an insoluble or "gel" fraction, consisting of the highly branched molecules and three-dimensional networks; and a soluble or "sol" fraction consisting of the more linear, low molecular weight molecules. Oxidative cross linking and scission of the molecules cause changes in the character and relative proportions of the sol and gel fractions of the polymer, which can be followed by various methods.

Cross linking will increase the gel fraction and increase the "tightness" (concentration of network junctures per unit volume) of the gel. Scission will decrease the gel fraction and make the gel "looser." When pieces of raw polymer

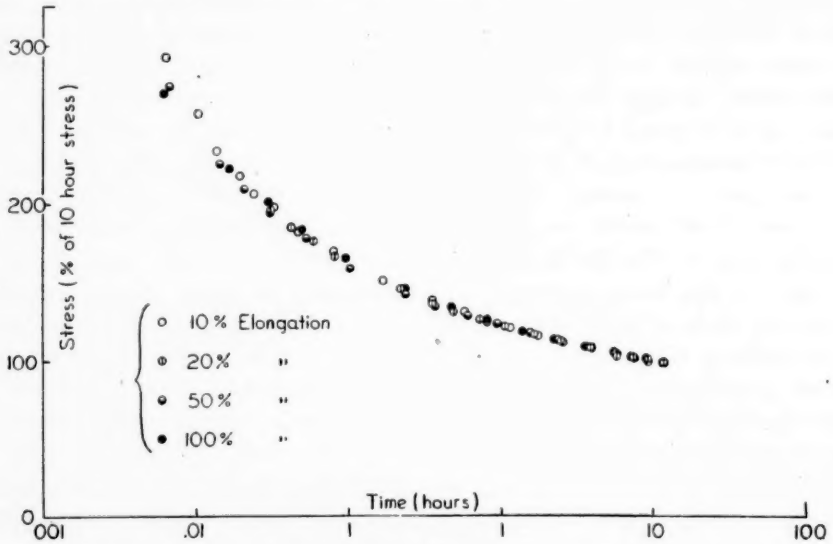

FIG. 21. Effect of elongation on low temperature stress relaxation, GR-S gum: −50°C.

are allowed to stand in benzene or toluene, the sol molecules go into solution, and the gel swells but does not dissolve. By weighing the swollen gel and measuring the concentration of the sol solution, the percent gel in the polymer can be calculated and also the "swelling index" of the gel (weight of swollen gel, rubber plus absorbed solution, divided by the weight of rubber in the gel), which should give a measure of the "tightness" of the gel. The average molecular weight of the sol molecules can be obtained by measuring the intrinsic viscosity of the sol solution. By making these measurements after various times of aging, the effects of cross linking and scission can be followed. Evaluating the softening and hardening of the raw polymer by hand test as aging progresses should provide a rough measure of the net effect of cross linking and scission, much as intermittent relaxation and creep measurements do. The rate of scission can be isolated almost completely by measuring the decrease in intrinsic viscosity of a rubber solution contained in a sealed viscosimeter. The solvent makes cross linking very difficult by keeping the molecules far apart, while the scission rate is unchanged; the action of the solvent is the same as described in the dissolution of vulcanizates, the effect being even greater here, however.

LOW TEMPERATURE SECONDARY BOND PHENOMENA

At low temperatures the secondary forces between chains and between portions of the same chain become sufficiently strong so that when the rubber is stretched many secondary interchain bonds do not relax during the stretching process and thus contribute to the measured initial stiffness of the rubber. These bonds will gradually relax, however, and reform in new positions which relieve the stress, so that if the rubber is maintained at constant elongation the stress will gradually decay until it approaches the equilibrium stress for that temperature as determined by the primary network (see Fig. 5).

Intermittent measurements of the stress required to attain a given elongation at low temperatures will give a constant value, provided that the rate of stretching is constant and that the rubber is undergoing no slow crystallization.

The effect of elongation on low temperature stress relaxation is shown in Fig. 21, where data for GR-S gum at −50°C are shown for four different elongations: 10 percent, 20 percent, 50 percent, and 100 percent.* Percent of 10-hour stress is plotted as the ordinate, to make the data readily comparable. It appears that in this range of elongations the relaxation curve obtained is independent of the elongation. For the very short time measurements, the 10 percent data are slightly above the others, but during the course of the curves as a whole no regular variation with elongation is found.

The relaxation of stress in rubbers maintained

* These data were sent us through the courtesy of Mr. I. B. Prettyman of the Firestone Physics Research Division.

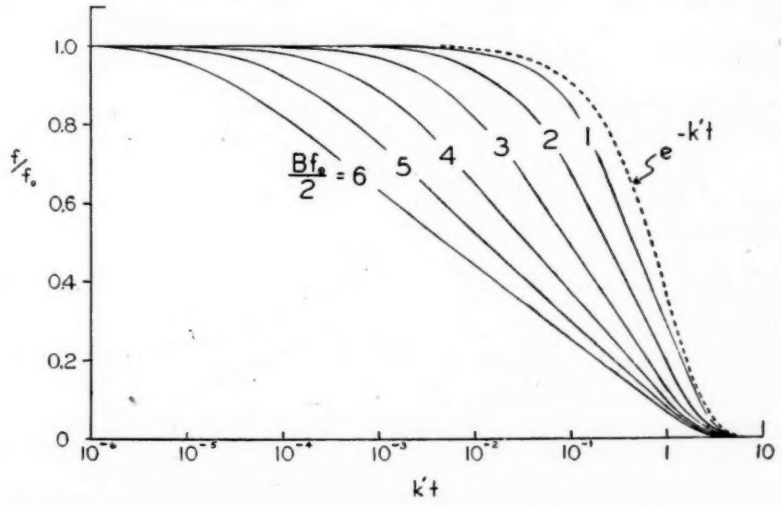

FIG. 22. Secondary bond relaxation (hyperbolic tangent decay).

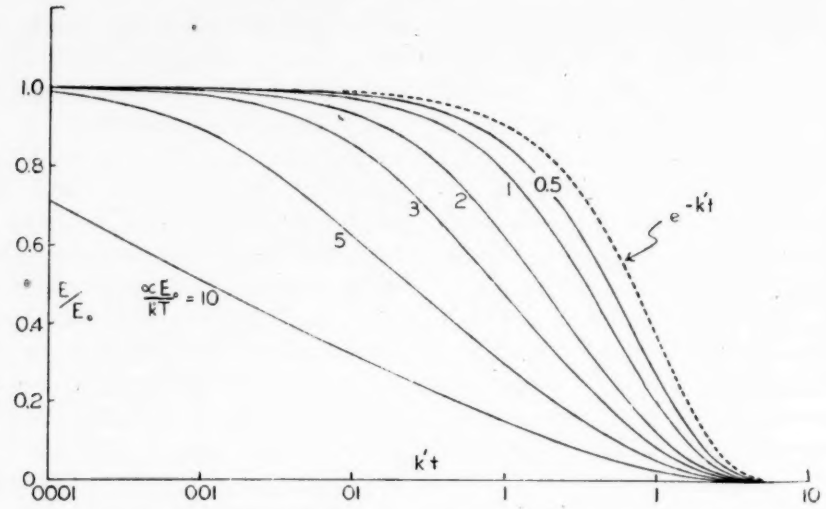

FIG. 23. Secondary bond relaxation (exponential integral decay).

at constant elongation at low temperatures does not follow the Maxwell decay law

$$f = f_0 e^{-t/\tau}, \tag{21}$$

where f is stress, t is time, f_0 = stress at time $t = 0$, and τ = relaxation time. Equation (21) is obtained by integrating Maxwell's equation (1) when $ds/dt = 0$. The Wiechert generalization of Maxwell's decay law gives

$$f = \sum_i (f_i)_0 \exp(-t/\tau_i), \tag{22}$$

where we assume a number of relaxation times or in the limit, a distribution of relaxation times. This mathematical result corresponds to a distribution of bond strengths, the relaxation behavior of each type of bond being governed by a linear relaxation law of the Maxwell type. For this case $(f_i)_0$ is the contribution of the ith type of bond to the stress at zero time and τ_i is the relaxation time for the ith type of bond. Equation (22) has the advantage of explaining naturally the fact that the stress decay curves for different

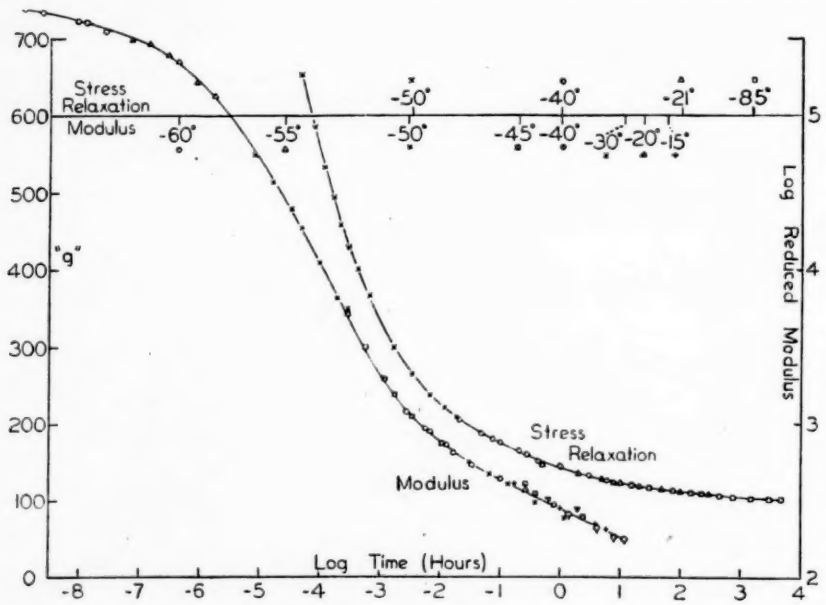

FIG. 24. Composite stress relaxation and composite low temperature modulus (GR-S gum).

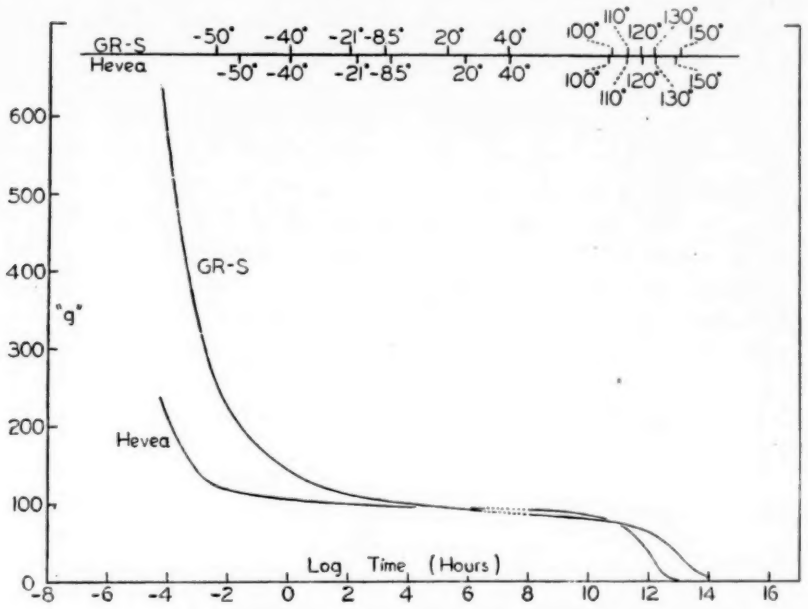

FIG. 25. Composite stress relaxation gum stocks.

elongations differ only by a scale factor (for elongations up to at least 100 percent) as discussed in the previous paragraph. This theory cannot be considered complete unless the actual distribution in relaxation times can be obtained from first principles. So far as agreement with experiment is concerned, any data can be fitted by a sufficiently complicated distribution of relaxation times.

Other possible relaxation laws exist, in particular the generalized Maxwell equation

$$\frac{ds}{dt}=\frac{1}{G}\frac{df}{dt}+n\lambda\frac{kT}{h}e^{-\Delta F^{\mp}/RT}2\sinh\frac{f\lambda}{2NkT}. \quad (23)$$

This equation is non-linear and the various quantities appearing in it have been defined previously. It may be written in the simplified form

$$\frac{ds}{dt}=\frac{1}{G}\frac{df}{dt}+A\sinh Bf, \quad (24)$$

where

$$A=2n\lambda\frac{kT}{h}e^{-\Delta F^{\mp}/kT},$$

and

$$B=\frac{\lambda}{2NkT}.$$

Integrating Eq. (24) for the case that $ds/dt=0$ the following expression is obtained:

$$\tanh\left(\frac{Bf}{2}\right)=\tanh\left(\frac{Bf_0}{2}\right)e^{-k't}, \quad (25)$$

where $k'=ABG$.

A graph of the hyperbolic tangent decay function is shown in Fig. 22, where f/f_0 is plotted against the logarithm of $k't$. The solid curves are the decay function for different values of $(Bf_0/2)$, and the dotted curve, included for comparison, is that of the simple first-order decay function

$$f=f_0e^{-k't}. \quad (26)$$

In order to explain by this theory the experimental fact that relaxation curves at different elongations differ only by a scale factor, it is necessary that $(Bf_0/2)$ be equal to a constant. Any reason why this should be is not known at present.

As a final example of a decay law that we may derive from *a priori* reasoning let us consider the dissipation of "non-equilibrium" energy. For constant extension experiments we shall assume that the stress and the extra stress energy (beyond the equilibrium value as determined by the primary network) are both functions of the number of secondary bonds that are

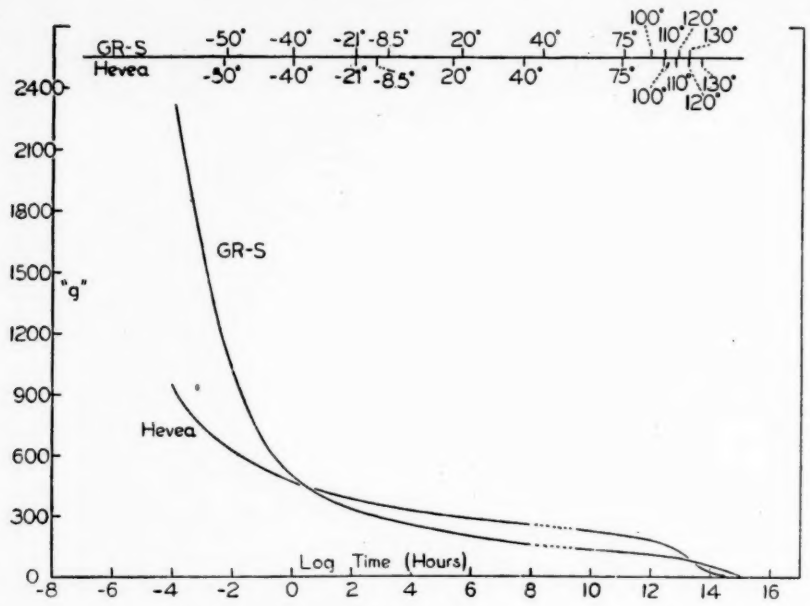

FIG. 26. Composite stress relaxation tread stocks.

holding in non-relaxed positions. In the unstretched state the interchain bonds form and reform in new relaxed positions without preference for either position. In the stretched state, however, the "extra" energy causes an asymmetry in the potential curve—in other words, there will be a net tendency for the bonds to move from stressed to relaxed positions with a concomitant dissipation of the excess stress energy. The equation derived from this picture is

$$-\frac{1}{E}\frac{dE}{dt}=k'\left[e^{\alpha E/kT}-e^{-(1-\alpha)E/kT}\right], \qquad (27)$$

where k' is the specific rate constant associated with the forming and reforming of secondary interchain bonds in the unstretched state, and α is equal to $\frac{1}{2}$ for symmetrical barriers. The integrated form of Eq. (27) (exponential integral decay) obtained by neglecting the second term in the bracket on the right-hand side is shown in Fig. 23. The stress is presumed to be related to the energy by some factor of proportionality inasmuch as the material is held at constant extension.

It is apparent that sufficient experimental work is not yet available to make a complete test of any of the theories presented here or elsewhere, although some interesting work has been done in this direction.[10] One of the difficulties is that at any given temperature, measurements extending over very many cycles of logarithmic time must be made to obtain a complete picture of the stress decay process.

COMPOSITE RELAXATION OF STRESS CURVES

To overcome the difficulty of obtaining experimental results over very extended times, it was observed that relaxation data (plotted in the form of "g" *versus* log t) obtained at one temperature could be superposed upon data obtained at another temperature merely by a translation along the log time axis. The reason for this is obvious in the case of the decay law

$$\text{"g"}=\text{"g"}_0e^{-k't}, \qquad (28)$$

which is obeyed by Hevea gum at high temperatures. The fact that the low temperature data can also be superposed in this way indicates that the time-temperature dependence of g follows a law of the kind

$$-dg/dt=\phi(T)\psi(g). \qquad (29)$$

How well low temperature data at different temperatures, either stress relaxation or modulus

[10] M. Mooney, W. E. Wolstenholme, and D. S. Villars, J. App. Phys. 15, 324 (1944).

(measured by the bending creep method of Dr. Liska), can be superposed by translation along the log time axis is shown in Fig. 24. Values of "g" and the logarithm of the reduced modulus are shown plotted against the log-time scale appropriate for −40°C. The origin of the log-time scale for each temperature is shown in the scale on top of the page. The one-hour value (log time equals zero) is marked for each temperature on this scale, and the log-time scale below can be used for each temperature merely by reference to the correct origin. The different types of points represent data at different temperatures.

By this method a single graph can be used to show the complete stress-temperature-time relations of a rubberlike substance. Figures 25 and 26 based on the same principle as Fig. 24 are complete "stress biographies" of the Hevea and GR-S gum and tread stocks studied. From these figures the complete stress-time-temperature behavior of these rubbers can be determined for times that would be impossible to attain experimentally. Even though "g," the reduced stress, is plotted only as 50 percent elongation data, the curves have greater generality because at different elongations these curves would be altered only by a scale factor in the ordinate.

It should be remembered that two processes are shown in these composite curves, primary and secondary bond relaxation, with very different activation energies, and therefore different temperature coefficients. For this reason it is to be expected that if the primary bond relaxation at two different temperatures is superposed, the secondary bond relaxation at the two temperatures will not be superposed in that position. Two composite curves are really needed, one for primary and the other for secondary bonds, with the time origin for each temperature marked on the log time abscissa of each. Then to obtain the complete relaxation curve at any temperature, one would slide the first graph along the second until the two log time origins for that temperature coincided. Dotted lines are used to connect the primary and secondary regions of the composite curves in Figs. 25 and 26 to indicate this—that a single continuous relaxation curve, including both primary and secondary relaxation regions, is not universal for all temperatures, simply by choosing the appropriate point along the log time scale as origin. The reason that a single curve was obtained in the graphs shown here was merely the result of the fact that, in most of the superposition, one or the other of the two relaxation regions was being superposed.

The conclusions stated in this section of course depend on the validity of the superposition procedure. It seems fairly clear at the present time that the superposition procedure is truly applicable at high temperatures (i.e., for the primary bond relaxation region). The position of the origin on the log time scale for any temperature can be calculated by use of Eq. (17). At low temperatures the data used overlapped only to a small extent, so that it was very difficult to tell whether the curves at different temperatures really would superpose completely. Low temperature data over more extended times are needed to check this. For this reason the conclusions expressed here must be regarded as only tentative at the present time.

ACKNOWLEDGMENTS

The authors wish to thank the Firestone Tire and Rubber Company and Princeton University for making possible our researches on fundamental physical properties of rubber. In particular we wish to thank Dr. H. S. Taylor of Princeton, and Drs. J. N. Street and J. H. Dillon and Mr. I. B. Prettyman of Firestone for the cooperation, encouragement, and useful advice they have tendered us.

THE JOURNAL OF CHEMICAL PHYSICS VOLUME 13, NUMBER 1 JANUARY, 1945

Rise of Temperature on Fast Stretching of Butyl Rubber*

S. L. DART AND EUGENE GUTH
University of Notre Dame, Notre Dame, Indiana

(Received August 21, 1944)

The rise of temperature on fast stretching of natural and synthetic rubber stocks was investigated recently by Dart, Anthony, and Guth (D.A.G.). Since then the experimental technique was considerably improved and the taking of data greatly simplified thereby. By D.A.G. emphasis was placed to record temperature rises of up to 15°C for extensions up to 700 percent by a fast galvanometer of moderate sensitivity. In the present work this high heat was investigated. In addition, however, a less fast but more sensitive galvanometer was employed to record changes of temperature as small as 0.001°C for 0–80 percent extension. In accordance with early work by Joule on natural gum (1859) it was found that also Butyl gum stocks show an initial cooling effect. This passes at a thermoelastic inversion point into a heating effect. In agreement with the recent theory by James and Guth the thermoelastic inversion point was found to depend solely upon the thermal expansion coefficient of the unstretched stock. The coefficient of thermal expansion was measured for Butyl stocks in the present work. Butyl tread stocks also show the thermoelastic inversion point. The work of D.A.G. showed that the rise in temperature on extension is a slowly rising function of the extension with a steep upward turn and almost linear continuation after the onset of crystallization. The samples were kept extended for a minute and then the cooling arising on retraction also measured. The negative of the cooling on retraction plotted against extension fall, according to the second law of thermodynamics as it should under the extension curve, but crosses it at the onset of crystallization. For Butyl gum stocks this crossing takes place at rather high (600 percent or more) extensions in agreement with x-ray work. More similarity was found between Butyl and Hevea tread stocks than between the corresponding gum stocks. Loading shifts the onset of crystallization to a range of smaller extensions. In addition to measuring the change of temperature on extension and retraction, the residual rise in temperature after an extension and immediate fast cycle retraction was also observed. This quantity is a measure of internal friction in Butyl rubber and is closely connected with rebound and free vibration tests. Summarizing, the method described has a twofold application for development work: 1. Changes of the temperature on extension and delayed retraction indicate in a simple manner the onset and progress of crystallization. 2. Changes of the temperature in a fast cycle give an estimate for internal friction. Both these applications will facilitate attempts to improve present synthetics.

INTRODUCTION

THE rise of temperature on fast stretching is one of the noteworthy characteristics of rubber stocks. If one stretches rapidly a Hevea gum band several hundred percent and applies it to the chin, one gets a direct sensory observation of the heat developed. This shows that the temperature must have been higher than that of the body, i.e., there must have been a temperature rise of 12–15°C. Surprisingly enough such a "high heat" was not observed, when the human lip was replaced by a supposedly more objective apparatus, namely, by a thermocouple in conjunction with a galvanometer. In addition, different authors reported different values for the heat rise—all much lower than at 15°C. Recent work in this laboratory by Dart, Anthony, and Guth[1] was done with a fast galvanometer. This work showed that the use of slow galvanometers was one reason why previous investigators could not observe "high heat." In addition, a survey of various types of natural and synthetic gum and tread stocks showed that the heat generated depends sensibly upon the type of stock used. This accounts for the disagreement among earlier investigators.

The work of Dart, Anthony, and Guth[1] showed that for gum stocks, the rise in temperature on extension is a slowly rising function of the extension. This slow rise is owing to the heat into which the work of stretching is transformed. For stocks which crystallize on stretching, the rise in temperature takes a steep upward turn and continues almost linearly after the onset of crystallization. This was found to be the case for Hevea and Neoprene. Hycar OR, on the other hand, did not show the upward turn in agreement with x-ray data, which do not reveal any crystallization for this type of synthetic. Now, for the case of Butyl gum stocks, x-ray data show that they

* Presented on June 23, 1944 before the Inaugural Meeting of the Division of High-Polymer Physics of the American Physical Society at Rochester, New York.

[1] Dart, Anthony, and Guth, Ind. Eng. Chem. **34**, 1340 (1942).

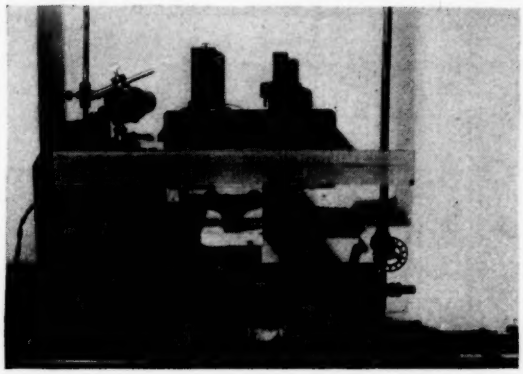

FIG. 1.

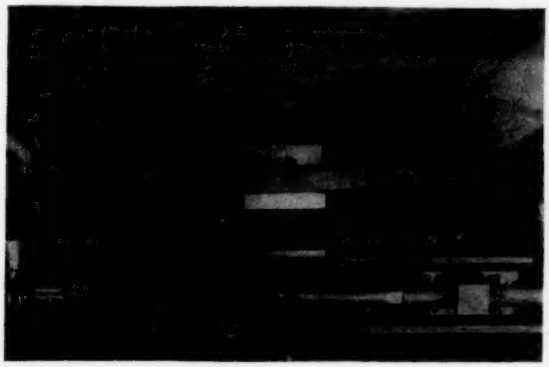

FIG. 2.

do crystallize on stretching, but start at very high extensions only (500 percent and higher). Therefore, it seemed to be of interest to study the onset and continuation of crystallization for Butyl stocks by means of "high heat" curves.

In addition the initial cooling effect at small extensions was studied by employing a sensitive but slower galvanometer. Changes of temperature as small as 0.001°C ("low heat") could be observed. The experimental technique for taking both high and low heat data was greatly improved and simplified compared to our earlier work referred to.[1] Moreover, besides taking extension and delayed retraction curves as in reference 1, the residual heat for extension and immediate retraction (fast cycle) was also observed.

I. EXPERIMENTAL METHOD

A compressed air driven machine was used to obtain rapid extensions and retractions. With this machine, extensions can be produced from 0 percent up to any elongation in 0.1 second. The machine can also be used for rapid extension-retraction oscillations up to frequencies as high as 600 per minute, and the gradual rise of temperature in the sample followed as a function of number of cycles, speed of cycles, and degree of elongation.

Temperatures were measured with a copper-constantan thermocouple sandwiched between two samples given a half-twist. For small temperature changes a galvanometer of longer period, about 8 sec., and a sensitivity of 4×10^{-9} amp. per millimeter was employed. This apparatus is shown in Figs. 1 and 2.

II. COMPOSITION OF THE STOCKS

The stocks were prepared for us by the Esso Laboratories. The ingredients of each vulcanizate are given in parts by weight in Table I. Numbers 1, 2, 4, and 5 were cured for 60 minutes at 307°F; number 3 (non-sulfur cure) for 45 minutes at 287°F. Slabs with dimensions $13.5\times13.5\times0.25$ were cured for 70 minutes.

III. PHYSICAL PROPERTIES OF THE RAW STOCKS AND TENSILE DATA FOR THE CURED STOCKS

The following data were communicated to us from the Esso Laboratories.

The Butyl A raw stock possessed about 0.95 mole percent (based on the C_4H_8 chain unit) of unsaturation according to the Kemp-Wijs method, the unsaturation figure for the Butyl B polymer is about 1.5 percent. Their intrinsic viscosities are about the same, 1.25 in di-isobutylene at 20°C. The corresponding viscosity average molecular weight is 290,000.

Tensile data for the cured stocks are given in Table II.

IV. RESULTS ON HIGH AND LOW HEAT

High heat curves for stocks 1–5 are given in Figs. 3–7. All three curves (extension, retraction, fast cycle) were obtained using one single sample. Previous work in this laboratory[1] has shown that somewhat higher ΔT values could be obtained by using a different sample for each extension, the reason being that some temporary or permanent set was introduced at each extension. However, variations within the batch partially offset this

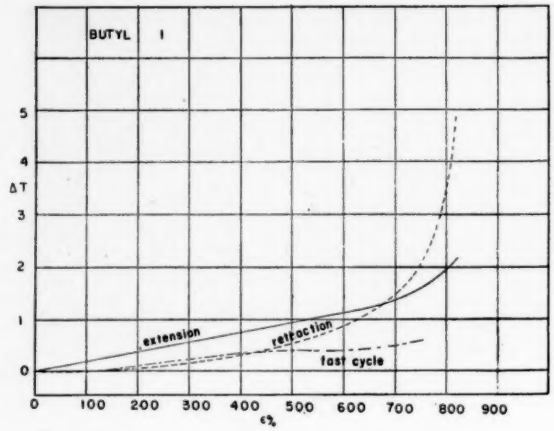

FIG. 3.

TABLE I.

Stock No.	1	2	3	4	5
Butyl A	100	100	—	—	—
Butyl B	—	—	—	100	100
Zinc oxide	5	5	—	5	5
Stearic acid	3	3	—	3	3
Sulfur	1.5	1.5	—	1.5	1.5
Calbot No. 9, Black	—	50	—	—	50
Treads	1	1	—	1	1
Captax	—	0.5	—	—	0.5

TABLE II.

Stock	Load at 300% lb./in.²	T.S. lb./in.²	B.E. in %
1	—	1900	950
2	280	2500	790
3	950	2000	500
4	—	2900	1000
5	380	2675	780

advantage of using different samples. The ΔT values obtained give the curve denoted "extension." After the sample had been stretched (in about one-tenth of a second), it was kept extended for one minute and then the machine pushed it back (again in one-tenth of a second) to the unstretched state. The negative of the temperature change involved in this (forced) retraction process is plotted as "retraction." The curve designated "fast cycle" represents the residual ΔT value for an extension and immediate (forced) retraction. Again, extension and retraction took place in two tenths of a second.

Low heat curves for stocks 4 and 5 are given in Figs. 8 and 9. Extension, retraction, and fast cycle curves were obtained in the same way as for the case of high heat.

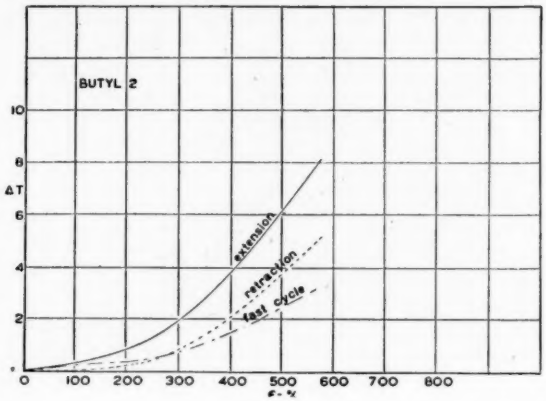

FIG. 4.

V. DISCUSSION OF THE RESULTS

The first question we have to answer is that concerning the basic physical significance of the extension, retraction, and fast cycle curves.

(a) Extension Curves

Thermodynamics (Kelvin, 1855) gives the formula for the change of temperature ΔT on adiabatic extension

$$\Delta T=\frac{T}{C_L}\int_1^L\left(\frac{\partial Z}{\partial T}\right)_L dL; \qquad (1)$$

where T is the absolute temperature, C_L the specific heat at constant length per cm³ (independent of L), L the relative length (extended length divided by original length, the original length taken at the initial temperature T), Z the stress (actual force per unit original cross section).

$$L=(\epsilon/100)+1 \qquad (2)$$

expresses L in terms of the more familiar percentage extension ϵ. Formula (1) correlates the temperature coefficient of the stress at constant extension $(\partial Z/\partial T)_L$ with the change in heat $\Delta T\cdot C_L$ on adiabatic stretching. The change (rise) in temperature on adiabatic stretching is entirely similar to the rise in temperature on adiabatic compression of a gas. The physical meaning of formula (1) is clearer if we recognize that (cf. Anthony, Caston, and Guth[2] and James

[2] Anthony, Caston, and Guth, J. Phys. Chem. **46**, 836 (1942); cf. also Peterson, Anthony, and Guth, Ind. Eng. Chem. **34**, 1349 (1942).

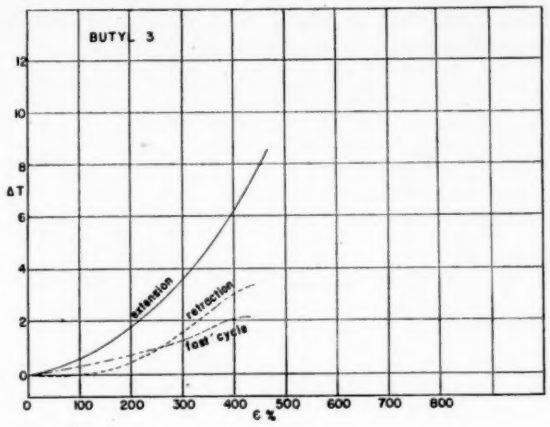

FIG. 5.

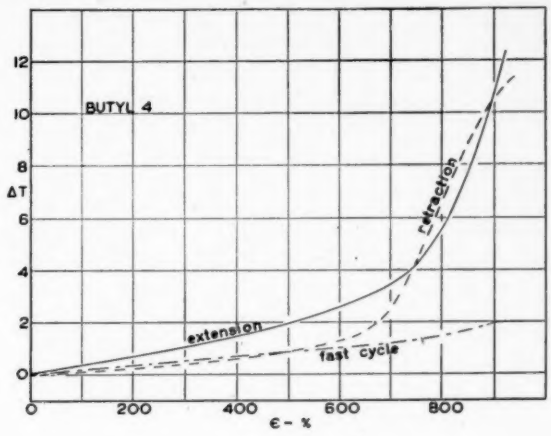

FIG. 6.

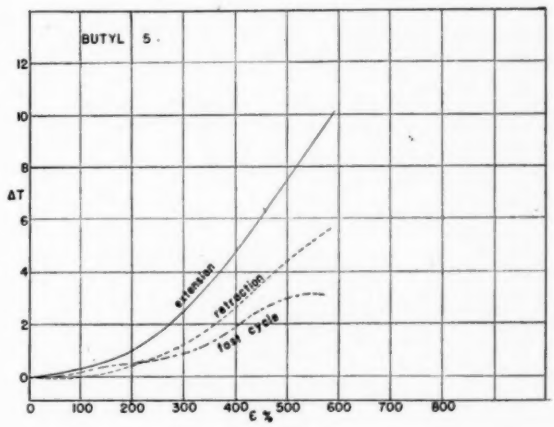

FIG. 7.

and Guth[3] for the use of this concept)

$$T(\partial Z/\partial T)_L = T(\partial S/\partial L)_T = Z_{(S)}. \qquad (3)$$

S is the entropy as a function of L and T, and $Z_{(S)}$ designates the entropy part of the stress. Then:

$$\Delta T = \frac{T}{C_L}\int_1^L Z_{(S)}dL \qquad (4)$$

or

$$(d/dL)(C_L\Delta T) = Z_{(S)}; \qquad (4')$$

i.e., differentiation of the ΔT *vs.* L curve yields $Z_{(S)}$ if C_L is known. If C_L is not known, (4′) will still yield $Z_{(S)}$ except for the numerical factor C_L.

The foregoing makes clear the physical significance of the ΔT *vs.* L curves for extension. Formula (4) is established first for a single phase. If a (more or less slow) crystallization process occurs in a certain L range, formula (4) holds also through crystallization.

The general behavior of $Z_{(S)}$ is known from references 2 and 3. There a relaxation method [described in reference 2] was applied to obtain $Z_{(S)}$. The range of crystallization was investigated by Wiegand and Snyder,[4] Meyer and Ferri,[5] Caston, Anthony, and Guth[6] and recently, more accurately by Wood and Roth.[7] From these investigations, it follows that the $Z_{(S)}$ *vs.* L curve looks schematically as drawn in Fig. 10. (a) is drawn to a larger scale than (b) in order to show clearly the thermoelastic inversion. Here we plotted, besides $Z_{(S)}$, the total stress Z and the internal energy component

$$Z_{(U)} = Z - Z_{(S)}. \qquad (5)$$

The integral of $Z_{(S)}$ as derived from Fig. 10 will appear as shown in Fig. 11 (assuming $C_L \cong 0.4$), i.e., the change in temperature is first negative, passes through a minimum, given by $(\partial Z/\partial T)_L = 0$, goes to zero and becomes positive.

$$(\partial Z/\partial T)_L = 0 \qquad (6)$$

defines the isometric (=isotonic) thermoelastic inversion point because, at the extension L_i, given by the root of (6), the sign of the slope of the isometrics (Z-T curves at constant L)

[3] H. James and E. Guth, J. Chem. Phys. **11**, 455 (1943); cf. also E. Guth, *Surface Chemistry*, pub. No. 21, A.A.A.S. (1943), p. 103; E. Guth, Alexander's *Colloid Chemistry*, (Reinhold Publishing Corporation, New York, 1944), Vol. V, p. 286.

[4] Wiegand and Snyder, Rubber Chem. Tech. **8**, 151 (1935).

[5] Meyer and Ferri, Helv. Chim. Acta. **18**, 570 (1935).

[6] Caston, Anthony, and Guth, unpublished material.

[7] L. A. Wood and F. A. Roth, J. App. Phys. **15**, 781 (1944). We are indebted to Dr. Wood and Mr. Roth for discussions of their work prior to its publication.

changes.

$$\Delta T=0 \tag{7}$$

defines the adiabatic thermoelastic inversion point, L_a. Both L_i and L_a are indicated in Fig. 10(a).

The statistical theory by James and Guth[3] gives an expression for $(\partial Z/\partial T)_L$ containing only one adjustable parameter K and the measurable cubic thermal expansion coefficient α of the unstretched sample (T_0: room temperature 300°K)

$$\left(\frac{\partial Z}{\partial T}\right)_L = K\left[L-\frac{1+\alpha T_0}{L^2}\right], \tag{8}$$

valid for the range of extension of Figs. 10(a) and 11(a). Inserting into (1) we obtain

$$\Delta T=(KT/2C_L)[L^2+L-2(1+\alpha T_0)] \times[(L-1)/L]. \tag{9}$$

From (8) and (6) we have

$$L_i=1+(\alpha/3)T_0; \tag{10}$$

from (9) and (7) it follows that

$$L_{ad}=1+(2\alpha/3)T_0. \tag{11}$$

We have measured α both for the gum and the tread stock and obtained

$$\alpha\text{-gum}=1.74\times10^{-4}, \tag{12}$$

$$\alpha\text{-tread}=1.17\times10^{-4}. \tag{13}$$

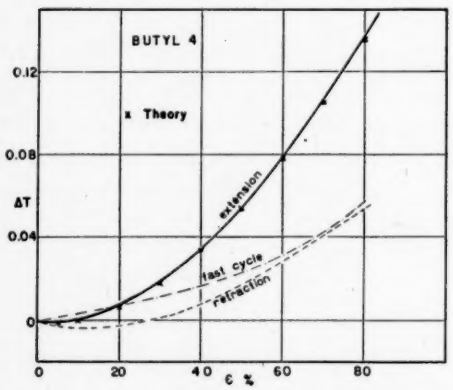

FIG. 8.

The value of α-gum looked somewhat low in view of the fact that for many Hevea and synthetic gum stocks $\alpha\cong2.1\times10^{-4}$. However, a glance at Fig. 8 shows that experimentally

$$L_i=1.05, \quad L_a=1.10, \tag{14}$$

which are just exactly the theoretical values according to (10) and (11) if we substitute (12). The crosses in Fig. 8 indicate the theoretical values for ΔT using again (12). The agreement with experiment is rather good.

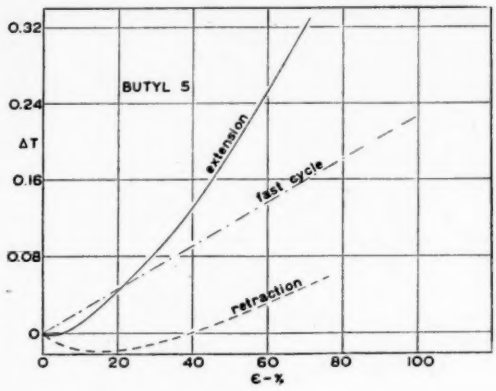

FIG. 9.

For extensions up to 700 percent the ΔT *vs.* L curves rise slowly. This whole range is covered by the statistical theory of James and Guth;[3] we just have to replace (8) by its generalization involving the inverse Langevin function.

Physically, in this range 0–700 percent the work done on stretching transforms practically completely into heat, $C_L\cdot\Delta T$.

For extensions above 700 percent, however, crystallization sets in. The $C_L\cdot\Delta T$ corresponding to the steep upward turn of the high heat curve represents the latent heat of crystallization. The above interpretation holds for gum stocks, i.e., Figs. 3 and 6. The tread stocks, Figs. 4 and 7 and the non-sulfur cure, Fig. 5, show different behavior. Here the high heat curve starts its upward turn much earlier. The early upward turn for tread stocks is partly owing to an earlier onset of crystallization as a consequence of carbon black reinforcement. Partly, however, it is owing to frictional heat between the rubber matrix and carbon black.

This interpretation for gum stocks is supported by considering the retraction curve.

(b) Retraction

The retraction curve is more arbitrary than the extension curve, since the one-minute delay could be replaced by a shorter or longer waiting

period, thereby changing the retraction curve. Below the range of crystallization the retraction curve is always below the extension curve in accordance with the second law of thermodynamics.

At the onset of crystallization the retraction curve crosses the extension curve, owing to the fact that additional crystallization took place during the waiting time of one minute. It was shown in reference 1 that the crystallization process takes time. After completion of crystallization, we have again one phase, and retraction recrosses the extension and is again below it. This may be seen in Fig. 6.

An estimate of the latent heat of crystallization may be obtained by taking the difference in ΔT between the two crossings. The difference in ΔT between the two crossings, multiplied by C_L, measures the heat of crystallization. We see from the steepness of rise of the extension and retraction curves that the heat of fusion is very considerable (cf. Fig. 6).

(c) Fast Cycle Curves

These curves give actually the hysteresis loop between the extension and retraction branch of stress-strain curves taken in 0.2 second. For, that loop is simply given by

$$\text{Loop} = C_L \cdot \Delta T. \qquad (15)$$

This loop (of Fig. 12) corresponds to the dynamic hysteresis loop for extensional free or forced vibrations around a static strain of $\epsilon^*/2$ and with a constant dynamic amplitude of $\epsilon^*/2$, and a

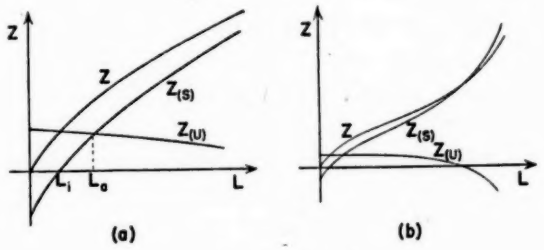

FIG. 10.

frequency of 5 cycles per second. It does correspond more closely to the first cycle of a free or a forced vibration. A comparison with sustained forced vibrations is possible, of course, by observing ΔT for repeated fast cycles. The relation of the fast cycle curves to rebound data is the same as that of the corresponding free vibrations. Of course, the static strains and amplitudes employed in forced or free vibrations are of the order of 10–30 percent, whereas the amplitudes

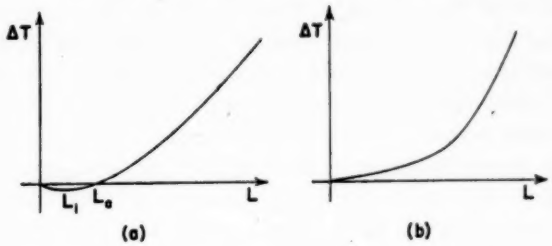

FIG. 11.

for high heat measurements may go right up to the breaking elongation, i.e., up to 1000 percent.

It should be pointed out that the impact resilience as measured by the rebound of a ball or of a pendulum depends *both* upon the dynamic hysteresis loop and upon the dynamic modulus, i.e., stiffness of the stock. Roughly, we may consider the rebound as a half free vibration. For the percentage resilience R we obtain then

$$R = (h_R/h) = \exp(-H_A/A^2E),$$

where h_R is the height of rebound, h is the height of fall, H_A is the energy loss per cycle for vibrations with constant amplitude A, and E is the dynamic modulus.*

We wish to point out that the hysteresis loops corresponding to fast cycles (0.2 sec.) are presumable solely or mostly owing to internal friction.

"Static" hysteresis loops, obtained with comparatively slow speed stretching (for instance, with the usual 20 inches per minute), are owing to stress relaxation. There is a correlation between the two types of hysteresis loops, but probably not a simple one. We shall discuss this correlation in another place.

The fast cycle curves are *not* the difference between extension and retraction. Particularly for the gum stocks the fast cycle curves increase much slower with the elongation than the extension and retraction curves. For small elongations, Fig. 8 shows the fast cycle to rise almost linearly in the beginning and then approach the retraction branch.

* Cf. for instance Dillon, Prettyman, and Hall, J. App. Phys. **15**, 309 (1944), see p. 320.

VI. GENERAL DISCUSSION

(a) Gum Stocks

1. Low Heat

The low heat curve for Butyl gum (compound 4) may be compared with that of a Hevea gum, cf. Fig. 5 of James and Guth.[3] The extension curves are about the same, both for Butyl and for Hevea. Since Butyl at the same elongation has a lower stress value than Hevea (i.e., the value of K is smaller for the former) the value of C_L must also be smaller for Butyl than for Hevea. This conclusion will be checked by direct measurement of C_L. The smaller value of the thermal expansion coefficient will also tend to raise ΔT, but this influence acts only in the neighborhood of the thermoelastic inversion point.

The retraction and fast cycle curves (the last not given in Fig. 5 of James and Guth[3]) differ greatly for Hevea and Butyl. Since Butyl shows less stress relaxation than Hevea, this difference must be owing to the considerably greater internal friction of Butyl.

2. High Heat

The extension curves for stocks in Figs. 3 and 6 have roughly the same form up to about 400 percent. It should be pointed out that the accuracy of high heat curves increases with the elongation because of the better contact between the rubber and the thermocouple. Above 400 percent the curve rises faster for stock 4 than for stock 1. This behavior is in keeping with the higher tensile strength and somewhat higher breaking elongation of stock 4 in contrast to stock 1. It is to be expected that between 800 and 1000 percent a further steep rise of ΔT occurs, in view of the steep rise of the stress-strain curves in this region. Experiments are underway to check this conclusion.

The retraction curves coincide for the two stocks up to about 600 percent elongation. From there on the curve for stock 4 rises steeper than that for stock 1.

The fast cycle curves rise very slowly for both stocks. The investigation of the range above 800 percent will be interesting.

Comparison of the Butyl high heat curves of Figs. 3 and 6, with the high heat curve of a Hevea gum stock (cf. Fig. 4 of Dart, Anthony, and Guth[1]) is quite revealing. That particular Hevea gum stock crystallizes at about 250 percent elongation, as the first crossing of the extension and retraction curves indicates. Actually the retraction branch is somewhat lower than the extension branch below 250 percent, as more accurate experiments have shown. However, the difference between extension and retraction is smaller for Hevea than for Butyl. The characteristic difference between Hevea and Butyl is, of course, the late and more abrupt crystallization of Butyl in contrast to the earlier and more gradual crystallization of Hevea. This is indicated in the schematic Fig. 13 where the solid curve represents extension and the dashed curve retraction. The first crossing indicates the onset of crystallization.

The correlation of stress-strain curves (and hysteresis loops) with x-ray data is somewhat complicated by the fact that x-ray diagrams are taken over a period of hours during which the rubber samples are kept at constant extension and suffer stress relaxation. No such difficulty enters into the discussion of crystallization using high heat data. As a matter of fact, high heat data may be helpful in establishing the correct relationship between x-ray and stress-strain data.

(b) Tread Stocks[8]

1. Low Heat

Figure 9 for stock 5 shows a thermoelastic inversion point and a much steeper rise of the low

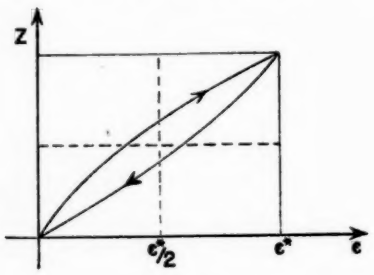

FIG. 12.

heat curve than Fig. 8 for the gum stocks. This steeper rise is, of course, caused by the stiffening

[8] For a theory of filler reinforcement cf. J. Rehner, Jr., J. App. Phys. **14**, 638 (1943). This aspect of the problem is discussed more fully by E. Guth, J. App. Phys. **16**, 20 (1945).

of the stock by carbon black reinforcement. The difference between extension and retraction branch is also much bigger for the tread than for the gum stocks. Butyl tread shows a low heat curve essentially similar to Hevea tread, the

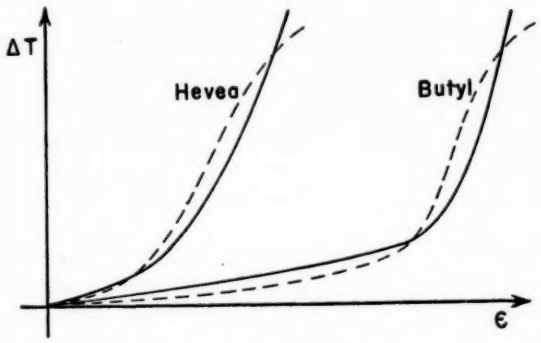

FIG. 13.

separation between extension and retraction branches being larger for Butyl than for Hevea.

2. High Heat

Figures 4 and 7 show the data for the stocks 2 and 5, respectively. Figure 5, the non-sulfur cure, shows essentially the behavior of a very stiff tread stock. For tread stocks, the retraction branch is always below the extension branch without any crossing. Conclusions about the onset of crystallization may be drawn only from the steepness of the curves. Therefrom one would conclude that crystallization starts between 200 and 300 percent. Figure 14 compares high heat curves for Hevea and Butyl tread. The cross on the curves indicates the onset of crystallization. The Hevea curve is taken from Fig. 7 of Dart, Anthony, and Guth.[1] Comparison of Figs. 13 and 14 shows that the carbon black induces both for Hevea and Butyl an earlier crystallization. Consequently stronger forces will act between the chains of a tread than for a gum stock. In order to get a correct view of carbon black reinforcement in Butyl rubber, it seems necessary to consider the whole stress-strain curve and the whole high heat curve, not just tensile strength. It was pointed out already by Turner, Haworth, Smith, and Zapp,[9] that on the basis of tensile strength alone, carbon blacks do not reinforce Butyl, but they enhance other physical properties, as for instance modulus and tear resistance. Figure 15 shows the stress-strain curves for stocks 4 and 5.

One sees that in the range 0–750 percent a reinforcement of the same degree takes place as for GR-S; actually, it is smaller for Butyl than for GR-S. This range is characterized by the absence of crystallization. It seems that a certain irregularity, suppressible by crystallization, is necessary for a specifically large reinforcement by carbon black. The fact that Butyl gum does crystallize appreciably beyond 750 percent, as evidenced by the abrupt rise in the high heat curve and in the stress-strain curve itself, does not count, so to say, since the black stock breaks at 780 percent. In Hevea, blacks also cause a decrease in the breaking elongation, but since the crystallization is more gradual, crystallization and carbon black add up, roughly speaking, in the reinforcement. Now for Hevea, the reinforcing effect is relatively larger for an undercure, than for the optimum cure (determined by maximum tensile), and relatively smaller for an overcure. The probable reason is that for an undercure the breaking elongation is higher and so crystallization and carbon black have a larger region to add up for reinforcement. From this point of view, it would be interesting to see how far an undercured Butyl stock may be reinforced by blacks. Although the undercured Butyl gum has a lower tensile than the optimally cured, the corresponding black stocks may reverse in the order, particularly, if the breaking elongation of the black stock could be extended, say over 900 percent. It should be pointed out, however, that the work of Turner, Haworth, Smith, and Zapp[9] (cf. their Figs. 5 and 6) does not indicate such a reversal.

Another possibility, to obtain higher black tensiles would be a shift of the range of crystallization to lower extension or to make it start earlier so that it would be more gradual and less abrupt.* The experimental methods described in this paper could be very helpful in such attempts to improve on Butyl.

VII. CONCLUSIONS

Study of the rise in temperature on fast stretching of Butyl gum and tread stocks throws

[9] Turner, Haworth, Smith, and Zapp, Ind. Eng. Chem. **35**, 958 (1943).

* Cf. Sturgis and Trepagner, Rubber Age **54**, 325 (1944).

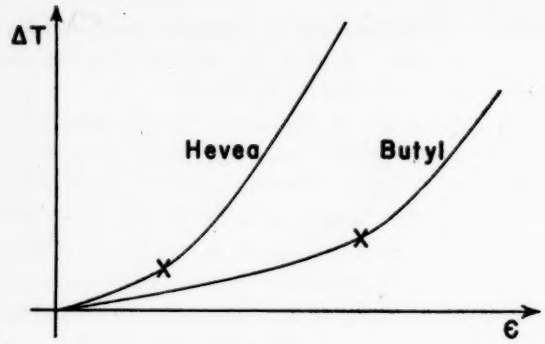

FIG. 14.

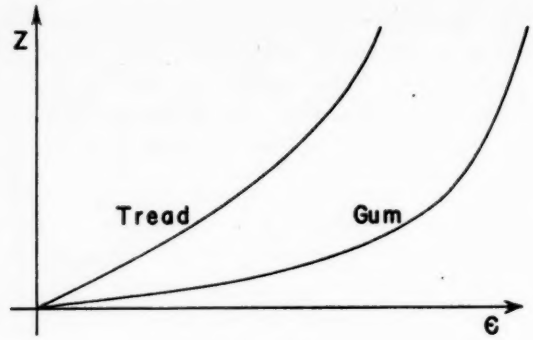

FIG. 15.

considerable light on crystallization, internal friction, and carbon black reinforcement as functions of elongation and other possible variables. For low elongations the low heat curves show the occurrence of thermoelastic inversion. They also show that internal friction is much larger for Butyl than for Hevea. For high elongations the high heat curves enable one to follow the late and abrupt crystallization, so characteristic for Butyl stocks. The carbon black reinforcement of Butyl is followed for the whole range of elongations up to the breaking point. Specific carbon black reinforcement takes place in the range of elongations before crystallization of the gum stock, but the shortening of the breaking elongation by the black excludes to a large extent the added reinforcement through crystallization.

Physical measurements of the type reported in this paper serve a manifold purpose. They enable one to establish a correlation between physical properties and chemical structure. Such a correlation is simpler for fundamental physical properties, as the ΔT *vs.* ϵ curve, than for the more complicated physical tests, as data from flexometer, which were designed to approach service conditions. Comparing different gum stocks with Butyl polymers, among themselves and with Hevea or other synthetics, these measurements may guide the development of better Butyl polymers. Finally, comparing tread with gum stocks they may help to recognize the nature of reinforcing by carbon blacks and the action of other compounding ingredients.

ACKNOWLEDGMENT

The authors wish to express their indebtedness to J. P. Haworth, John Rehner, Jr., and P. J. Flory of Esso Laboratories for the preparation of the samples used in this study, for the physical test data, and valuable discussions on Butyl rubber.

Comparison of the Structures of Stretched Linear Polymers*

MAURICE L. HUGGINS
Eastman Kodak Company, Rochester, New York

(Received August 7, 1944)

Published x-ray data from crystalline selenium and tellurium and from stretched sulfur (amorphous), polyethylene, polyisobutylene, polyvinyl alcohol, polyvinyl chloride, polyvinylidine chloride, polyoxymethylene, polyoxyethylene, polyethylene disulfide, polyethylene tetrasulfide, and polyphosphonitrile chloride are compared. In most cases the experimental identity distance in the direction of the chain axes and the expected interatomic distances and interbond angles are found to be in agreement with the assumption that the chain atoms form a regular spiral, unidirectional in each chain and of uniform pitch. Apparent exceptions are briefly discussed.

X-RAY diffraction data show that substances composed of long chain molecules, when stretched, if not otherwise, tend to form crystalline arrangements in which the chain axes lie parallel to each other. In some cases, as in polyethylene,[1] polyvinyl alcohol,[2-4] and polyvinyl chloride,[3] the data indicate a planar zigzag arrangement of the chain atoms in each chain (Figs. 1 and 2). Each chain is extended as far as possible, consistent with the maintenance of the expected bond distances (~1.53A for C—C) and bond angles (~110° for ∠C—C—C). In most instances, however, the data are not in agreement with such a structure. The number of chain atoms between like points in a chain is greater than two and the "identity distance"—the distance between consecutive like points—differs from what would be expected for a plane zigzag arrangement. In this paper, the structures of these substances are discussed.

In accordance with well-established principles of structural chemistry, we should expect a chain composed of chain atoms which are equivalent as regards the atoms to which they are bonded to assume a structure (on crystallization) in which these chain atoms are in crystallographically equivalent positions. This requirement is satisfied by a planar zigzag structure or by a unidirectional spiral structure of uniform pitch. Which type is assumed in a given case (and the constants of the spiral, if the latter) will depend upon intra- and interchain forces, as discussed below.

Polyethylene,[1] $(—CH_2—)_n$, and crystalline "metallic" selenium[5,6] and tellurium[5,6] are composed of chain molecules in which the chain atoms (C, Se, Te) are all equivalent. In polyethylene, the chains have the planar zigzag structure; in selenium and tellurium, the chains are

* Presented on June 24, 1944 before the Inaugural Meeting of the Division of High-Polymer Physics of the American Physical Society at Rochester, New York. Communication No. 986 from the Kodak Research Laboratories.

[1] C. W. Bunn, Trans. Faraday Soc. **35**, 482 (1939).
[2] F. Halle and W. Hofmann, Naturwiss. **23**, 770 (1935).
[3] C. S. Fuller, Chem. Rev. **26**, 143 (1940).
[4] R. C. L. Mooney, J. Am. Chem. Soc. **63**, 2828 (1941).
[5] M. K. Slattery, Phys. Rev. **21**, 378 (1923); **25**, 333 (1925).
[6] A. J. Bradley, Phil. Mag. **48**, 477 (1924).

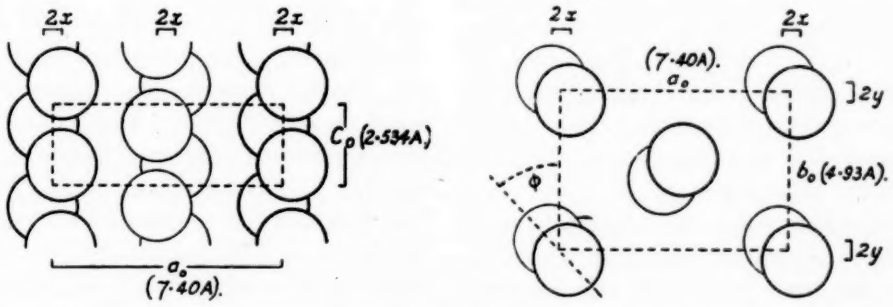

FIG. 1. Distribution of zigzag carbon chains in polyethylene, $(—CH_2—)_n$, according to Bunn (reference 1).

TABLE I. Data for various polymer structures.

Polymer	Repeating unit	Identity distance (l)	Bond distance (assumed)	Bond angle (calc.)	No. of chain atoms per identity distance (m)	No. of revolutions per identity distance (p)	Rotation per chain bond (α)	
Polyethylene	—CH_2—	2.534A	1.53A	112°	2	1	180°	
Selenium	—Se—	4.95	2.32	105°	3	1	120°	
Tellurium	—Te—	5.91	2.86	102°	3	1	120°	
Sulfur	—S—	9.26	2.12	{107° {107°	8 6	2 2	90° 120°	Reverse ? Reverse ?
Polyvinyl chloride		5.0	1.53	110°	4	2	180°	
Polyvinyl alcohol		2.52	1.53	110°	2	1	180°	
Polyisobutylene		18.63	1.53	111°	16	7	157.5°	
Polyvinylidene chloride		4.67	1.53	122°	4		Not a uniform spiral	
Polyoxymethylene		17.3	1.43	111°	18	5	100°	
Polyoxyethylene		19.5	C—C 1.53 C—O 1.43	{108° {110° (assumed)	24 27	6 5	90° non-uniform spiral	Reverse ? ?
Polyphosphonitrile chloride		4.92	1.65	124°	4	1	90°	
Polyethylene disulfide		8.8	1.825 (Av.)	111°	8	2	90° (Av.)	Reverse ?
Polyethylene tetrasulfide	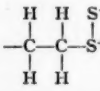	4.32	1.825 (Av.)	110°	4	1	90° (Av.)	

uniform spirals with three chain atoms per identity distance (Figs. 3[7] and 4). The bond distances and bond angles (Table I) agree with what would be expected from structure theory and from our knowledge of corresponding distances and angles in the substances.

A planar zigzag structure can be considered as a special case of a uniform spiral, in which for each bond in the chain there is an angular rotation (α) of $360°/2$ and a translation of $t/2$, where t is the identity distance. In selenium or tellurium, the angular rotation and translation per chain bond are $360°/3$ and $t/3$, respectively. In general, for a uniform spiral, there is, per chain bond, an angular and translational shift of magnitudes $p360°/m$ and t/m, respectively, where p and m are integers. From x-ray data, t and m may be deduced. Knowing these, one can compute a value of α corresponding to any pair of assumed values of bond distance and angle. If p, computed

[7] Strukturbericht **1**, 27 (1931).

from the equation

$$p = \alpha m/360°,$$

is found to be approximately integral, values of bond distance and angle close to those assumed are consistent with the assumption of a uniform spiral and with the experimental t and m values. By assuming p to be *exactly* integral, one may then compute the exact value of bond angle consistent with the observed t and m values and an assumed bond distance. This procedure was followed in deducing the bond angles in Table I. (Alternatively, one might assume bond angles and deduce bond distances.)

The data on fibrous sulfur should be mentioned. Meyer and Go[8,9] have deduced unit cell dimensions, including a fiber period of 9.26A, and suggested (on the basis of very meager evidence) that there are 14 chains of 8 S atoms, each passing through this cell. Meyer later proposed, as an alternative, 16 chains of 8 atoms each. The published data seem to be in as good or better agreement with 18 chains of 6 atoms each. Either 8 or 6 atoms per 9.26A in the fiber direction would be consistent with the assumption of uniform spirals if one permits *two* complete rotations per identity distance (see Table I). The doubled identity distance could be accounted for by assuming a reversal of direction of the helix after each complete rotation (Fig. 5). Obviously, a more detailed structure analysis is required.

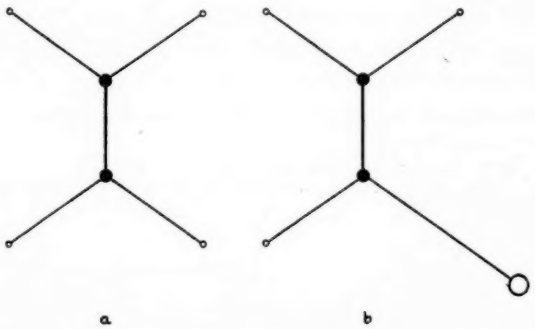

FIG. 2. Projections of proposed structures for polyethylene (a) and polyvinyl alcohol (b). The hydroxyl hydrogen atoms of the latter are not shown. Polyvinyl chloride is presumed to have a structure like (b), but with the Cl atoms of the CHCl groups alternating from one side to the other of the plane of the C—C zigzag.

[8] K. H. Meyer and Y. Go, Helv. Chem. Acta **17**, 1081 (1934).

[9] K. H. Meyer, *Natural and Synthetic High Polymers* (Interscience Publishers, Inc., New York, 1942), p. 51.

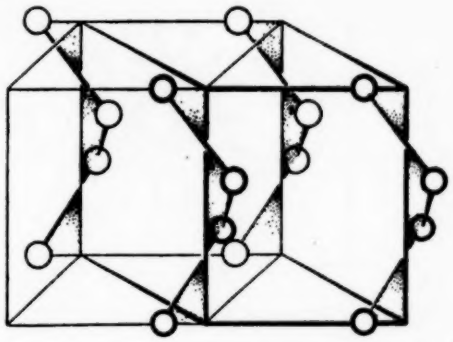

FIG. 3. The structure of Se and Te crystals. From the *Strukturbericht* (reference 7).

Plane zigzags or uniform spirals are also necessary when alternate chain atoms are different with respect to their attachment to other atoms, as in vinyl polymers, if all the bonds in a chain are equivalent. Interaction between the groups attached to the chain atoms within each chain or between neighboring chains may, however, make another arrangement more stable. (See the discussion of polyvinylidene chloride below.)

Polyvinyl chloride[3] and polyvinyl alcohol[2–4] give x-ray data agreeing with a plane zigzag structure having the customary C—C distances and ∠C—C—C bond angles. The identity distance in polyvinyl chloride is approximately twice that in polyvinyl alcohol. As pointed out by Fuller, the larger value would be expected if the chloride atoms are alternately placed, first on one side and then on the other, with respect to the plane of the zigzag (Fig. 2).

X-ray data from polyisobutylene have been interpreted by Fuller, Frosch, and Pape[10] as showing 16 chain atoms per fiber period, 18.63±0.05A. These figures are in agreement with the assumption of a uniform spiral with tetrahedral bond angles and the usual C—C distance. The angular shift α is 157.5°. The departure from a plane zigzag structure, for which $\alpha = 180°$, is thus not very great (Figs. 4 and 6).

Reinhardt[11] has reported a fiber period of 4.67A for polyvinylidene chloride with 4 chain atoms (two residues) per unit in each chain. These data are not in accord with a uniform spiral structure. The arrangement (Fig. 7) he proposes is a reasonable one, although it is neces-

[10] C. S. Fuller, C. J. Frosch, and N. R. Pape, J. Am. Chem. Soc. **62**, 1905 (1940).

[11] R. C. Reinhardt, Ind. Anal. Chem. **35**, 422 (1943).

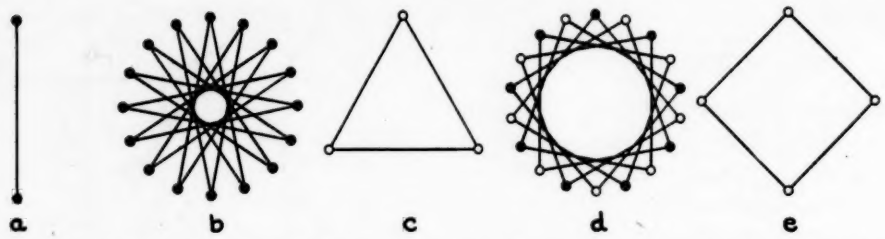

FIG. 4. Projections of the chain atoms and bonds in certain structures, assuming uniform spirals. (a) Polyethylene, polyvinyl alcohol, polyvinyl chloride. (b) Polyisobutylene. (c) Selenium, tellurium. (d) Polyoxymethylene. (e) Polyphosphonitrilechloride, polyethylene tetrasulfide.

sary to assume a C—C—C bond angle greater than 120°. The type of arrangement can be attributed to strong interaction between the side atoms, H and Cl, of opposite polarity.

In polyoxymethylene, $(-CH_2-O-)_n$, as in the vinyl polymers, the chain atoms are alternately of two types: Both OCO and COC bond angles would be expected to be in the neighborhood of "the tetrahedral angle." The C—O distance should be about 1.43A. These expectations and the experimental value[12,13] of the fiber period, 17.3A for 9 $-CH_2O-$ groups (18 chain atoms), agree with the assumption of a uniform spiral (Table I and Fig. 4).

In polyoxyethylene or polyethylene oxide $(-CH_2-CH_2-O-)_n$, the chain bonds are not all alike. The assumption of a uniform spiral, with the expected bond distances and with all bond angles in the neighborhood of 110°, leads to an identity distance just one-third of the experimental value.[14] There is no obvious reason for this discrepancy. It is likely that in this case the assumption of a spiral of uniform slope is in error. There is no symmetry argument for it, and it is certainly reasonable to expect better packing and greater stability for a structure in which the slope of the C—C bonds differs from that of the C—O and O—C bonds. Assuming a unidirectional spiral with slopes of C—O and O—C bonds the same and with 110° bond angles throughout, the observed identity distance[12] is found to correspond to 5 revolutions of the chain, with the C—C bonds nearly parallel to the spiral axis (the projection of the 1.53A bond distance on the axis is 1.48A) (see Fig. 8). This differs considerably from the meandering structure assumed by Sauter,[13] in which the C—C bonds are roughly perpendicular to the chain axis.

Sauter's conclusion that there are 9 $-CH_2-CH_2-O-$ residues per identity distance, in the polyoxyethylene structure, is questionable.[15] If there should really be only 8 such residues per identity distance, a reverse spiral of uniform slope would be possible. [See Table I and Fig. 6(b).] Further structure work is obviously necessary.

Polyphosphonitrile chloride is another substance which consists of chain molecules in which the chain atoms are alternately of two types. The structure can be considered as resonating, according to the scheme

$$\left(-N=\underset{Cl}{\overset{Cl}{P}}-\right)_n \leftrightarrow \left(=N-\underset{Cl}{\overset{Cl}{P}}=\right)_n .$$

The distance between adjacent N and P atoms can be taken as 1.65A, the value found by Brockway and Bright[16] for the trimer, a ring compound, by electron diffraction methods.

[12] J. Hengstenberg, Ann. d. Physik [4] **84**, 245 (1927).
[13] E. Sauter, Zeits. f. physik. Chemie **B18**, 417 (1932); **B21**, 186 (1933).
[14] E. Sauter, Zeits. f. physik. Chemie **B21**, 161 (1933).
[15] Cf. Meyer, reference 9, p. 196.
[16] L. O. Brockway and W. M. Bright, J. Am. Chem. Soc. **65**, 1551 (1943).

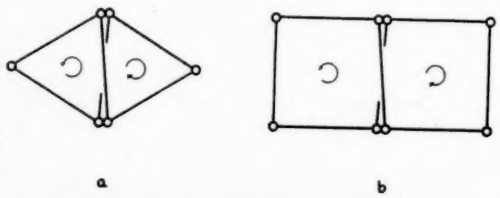

FIG. 5. Projections of two possible reverse spiral structures for fibrous sulfur. So as to show better the spiral arrangements, the projections of the middle atoms, in both structures, have been shifted slightly from their true positions. A structure of the type of (b) may also be correct for polyoxyethylene and polyethylene disulfide.

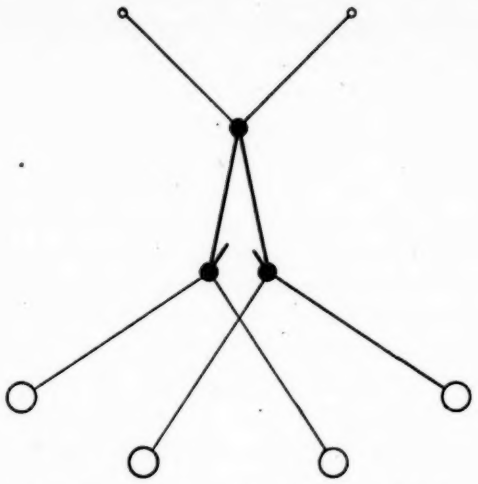

FIG. 6. Projection of a small section of a polyisobutylene spiral. Large circles denote carbon atoms of methyl (CH_3) groups.

Meyer, Lotmer, and Pankow,[17] in their x-ray study of the polymer, deduced 4.92±0.05A for the fiber period and concluded that there are 4 chain atoms in this distance. From these results,

[17] K. H. Meyer, W. Lotmar, and G. W. Pankow, Helv. Chem. Acta **18**, 930 (1936).

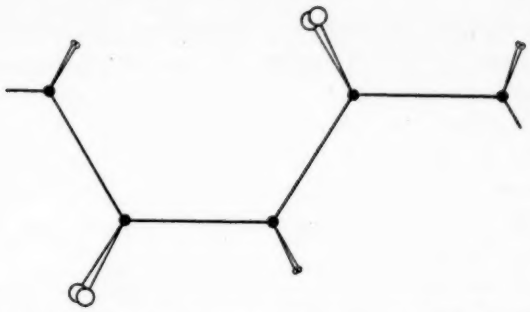

FIG. 7. Projection of the polyvinylidene chloride structure onto the plane of the —C—C— chain, according to Reinhardt. The positions of the H and Cl projections have been displaced slightly.

the assumption of a uniform spiral leads to an average bond angle, ∠PNP or ∠NPN, of 124° (Table I and Fig. 4). This is reasonable, being close to 125° 16′, the calculated angle between a single and a double bond for regular tetrahedra. In the trimer ring, the average angle is about 120°.

In polyethylene disulfide, $(—CH_2—CH_2—S—S—)_n$, and polyethylene tetrasulfide,

$$\left(—CH_2—CH_2—\overset{\overset{S}{\|}}{S}—\overset{\overset{S}{\|}}{S}—\right)_n,$$

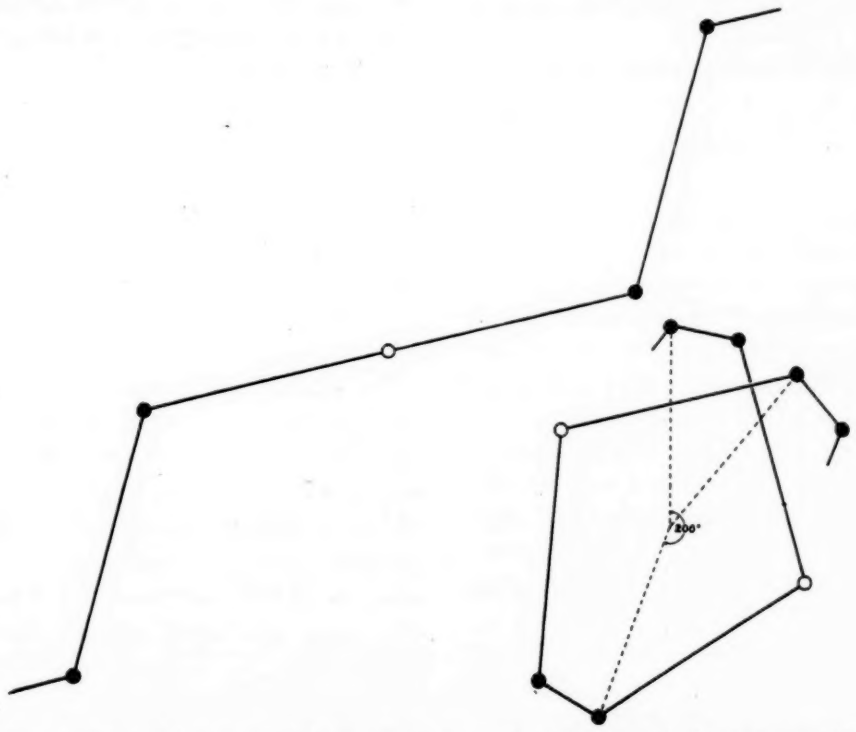

FIG. 8. Illustrating a possible structure for polyoxyethylene (polyethylene oxide), $(—CH_2—CH_2—O—)_n$. A projection of a portion of the helical chain is shown at the lower right. Above and to the left is the arrangement obtained by unrolling the helix onto a plane; this shows the different pitch of the C—C and C—O—C portions of the chain.

as in polyoxyethylene, symmetry and similar arguments do not require uniform slopes for the chain bonds. Nevertheless, the observed fiber distances[3,18] are in agreement with the assumption of spirals of uniform pitch with approximately tetrahedral bond angles (see Table I and Figs. 4 and 5)—a reverse spiral in the case of the disulfide.

With regard to rubber, guttapercha, polychloroprene, polyamides, polyesters, and other substances composed of chains more complex than those already considered, we might expect uniform, or nearly uniform, spirals except when prevented by strong atomic interactions (other than those determining the bond distances and angles), either within the same chain or between chains. Detailed consideration of these structures will not be attempted at this time.

The angular shift per chain atom in a molecular spiral may be determined primarily by the requirements for most stable (lowest energy) packing of the chain molecules in the mass or by forces between atoms in the same chain. In addition, if the substance is held under tension, there is the stretching force tending to extend the chain in the direction of its axis as much as possible. If not prevented by other forces, this stretching force produces a plane zigzag arrangement—the most extended one possible for given bond angles and distances. Intrachain forces may make this structure impossible, as, for instance, in the case of polyisobutylene, in which repulsion between the methyl groups on alternate carbon atoms forces a small angular shift of these atoms around the chain axis (Fig. 6). In a case such as selenium or tellurium, the form of spiral is probably largely determined by forces between atoms in different chains, tending to produce an arrangement of atoms as closely packed as possible consistent with the maintenance of stable bond distances and angles.

In conclusion, it must be emphasized that most of the structural arrangements which have been discussed require further experimental confirmation. Work along this line is planned by the writer when war conditions permit. In the meantime, it must be considered interesting and probably significant that, of the variety of simple polymer structures for which identity distance data are available, nearly all are in accord with the simple reasonable hypothesis of uniform spiraling.

[18] J. R. Katz, Trans. Faraday Soc. **32**, 77 (1936).

THE JOURNAL OF CHEMICAL PHYSICS VOLUME 13, NUMBER 1 JANUARY, 1945

The Influence of Velocity Gradient on the Relation Between Viscosity and Concentration in Cuprammonium Solutions of Cellulose*

W. James Lyons
*Southern Regional Research Laboratory,** New Orleans, Louisiana*
(Received August 4, 1944)

The numerous equations which have hitherto been employed to relate the viscosity of solutions of high polymers to the concentration of the solute have neglected to recognize explicitly the influence which velocity gradient (rate of shear) has upon the observed viscosity of non-Newtonian liquids. Consequently, the theoretically important, intrinsic viscosity, calculated on the basis of these equations, from data obtained on a solution in the anomalous region, is found to have a different value for each velocity gradient prevailing during measurement. A modification of the Baker-Philippoff equation has been developed empirically having the advantage that it yields a uniform value for the intrinsic viscosity of a given solution regardless of changes in velocity gradient. This new equation:

$$\eta_r=\left(1+\frac{c}{\lambda}\right)^8+\left(k_i-\frac{8}{\lambda}\right)c,$$

has been found to agree well with data on cuprammonium solutions of cellulose in concentrations below 0.5 g per 100 ml. The parameter λ, interpreted as a function of velocity gradient, is found to increase with gradient, while k_i, which is shown to be the intrinsic viscosity η_i, is found to have a constant value characteristic of the solute. It appears that the second constant appearing in other recent equations in addition to the intrinsic viscosity, may be interpreted as a velocity gradient adjustment term. The algebraic series into which the various recent equations can be expanded to express η_r are strikingly similar to each other and to a proposed equation based on the Eyring reaction-rate theory.

INTRODUCTION

THE employment of viscometry for the reliable determination of molecular weights depends upon the determination of a quantity which characterizes the viscous nature of the substance under study irrespective of experimental conditions. Among the important conditioning factors affecting the viscosity of solutions of high-polymeric substances are concentration and velocity gradient (rate of shear). Most attention during the past decade has been focused on the relationship between viscosity and concentration, the tendency being to emphasize zero concentration as the definitive condition for the characteristic viscous constant. Both viscosity and concentration appear explicitly in the analytical expression of the Staudinger theory. In the calculation of the intrinsic viscosity

$$\eta_i\equiv\lim_{c\to 0}\frac{\eta_{sp}}{c},$$

where $\eta_{sp}=\eta_r-1=$specific viscosity, $\eta_r=$relative viscosity, and $c=$concentration, it is generally assumed that the solution behaves as a normal, Newtonian liquid. Many solutions of high polymers, such as cellulose in cuprammonium hydroxide, however, exhibit anomalous behavior in that the apparent viscosity, instead of remaining constant at a given concentration, varies with the velocity gradient prevailing during measurement. In analogy with the treatment of the concentration effect, attempts have been made to evaluate the viscosity at zero velocity gradient, in order to nullify the velocity gradient effect, but these attempts have not been successful.

The neglect of the velocity gradient effect is somewhat justifiable if, as is frequently the case in molecular-weight studies, very low concentrations are employed. Under this circumstance, as

* Presented on June 24, 1944 before the Inaugural Meeting of the Division of High-Polymer Physics of the American Physical Society at Rochester, New York.

** This is one of the laboratories of the Bureau of Agricultural and Industrial Chemistry, Agricultural Research Administration, U. S. Department of Agriculture.

was recognized some years ago by Staudinger,[1] the anomalous behavior becomes quite obscure, if not negligible, in many high-polymer solutions. An illustration of the diminishing importance of velocity gradient as the concentration decreases is afforded by Fig. 1, in which are plotted values of the relative viscosity for various values of D_P, the velocity gradient which appears in the development of the Poiseuille equation.* While the differences between relative viscosities at the various gradients apparently vanish at the lowest concentrations, the graph clearly suggests that in this sample, Co-159, the small differences are merely masked by experimental error, and that the anomalous effect prevails down to zero concentration. Similar data for the other cellulose sample, Co-1374, are plotted in Fig. 2, for the limited region of low concentrations. Here the consistency of the relative positions of the experimental points for the different D_P's at each chosen concentration indicates a real, even though a small, anomalous effect. Table I brings out more clearly the character of the small differences in η_r which are involved in the interpretation of the data for low concentrations.

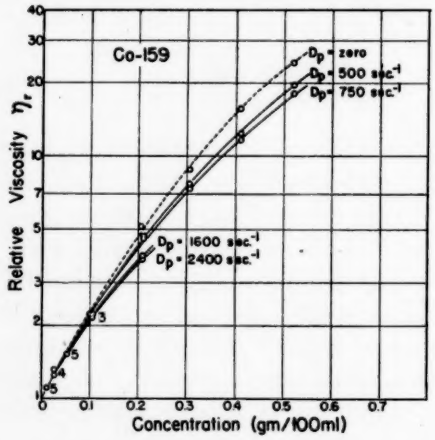

FIG. 1. Relative viscosity *vs.* concentration for a purified cotton cellulose, Co-159, dispersed in cuprammonium hydroxide, showing different values of η_r found at particular concentrations, depending on the velocity gradient D_P employed. The numerals beside certain plotted circles indicate the number of experimental values represented by each circle.

That dilution evidently does not remove the anomalous behavior in high-polymeric solutions has also been shown by Conrad,[2] using data of Staudinger for very low concentrations of nitrocellulose in Butyl acetate.

Undoubtedly the families of curves of the type in Fig. 2 converge exactly to a common value of η_{sp} *at infinite dilution*. Thus we may arrive at the same value for a measure of the viscous character of the solution as we would have attained had we been able to evaluate accurately the viscosities at zero velocity gradient for various concentrations, and to extrapolate these values to infinite dilution. From the above considerations it is evident, however, that while at infinite dilution the velocity gradient ceases to be a pertinent variable, the functional relationship between viscosity and concentration differs with each velocity gradient used in experiment.

The numerous equations which have been proposed relating the viscosity to the concentration of a solution have been assembled and compared by Mark[3] and by Pfeiffer and Osborn.[4] Of special interest in the present discussion is Philippoff's[5] development of Baker's formula:

$$\eta_r = (1 + c/c_0)^8, \tag{1}$$

where c_0 = a characteristic constant. Also of interest is the equation advanced by Schulz and Blaschke[6] and Huggins,[7] *viz.*:

$$\frac{\eta_{sp}}{c} = \eta_i(1 + k'\eta_{sp}), \tag{2}$$

and the equation proposed by Martin:[8]

$$\log \frac{\eta_{sp}}{c} = \log \eta_i + K\eta_i c. \tag{3}$$

[1] H. Staudinger, Papier-Fabr. **36**, 473 (1938), especially pp. 478–9.

* In the Poiseuille equation the velocity gradient D_P is $(4V/\pi r^3 t)$. This quantity is to be distinguished from the *mean* velocity gradient which is given by the expression $(8V/3\pi r^3 t)$, and is frequently used.

[2] C. M. Conrad, Ind. Eng. Chem. Anal. Ed. **13**, 526 (1941).

[3] H. Mark, *Physical Chemistry of High Polymeric Systems* (Interscience Publishers, Inc., New York, 1940), p. 293.

[4] G. H. Pfeiffer and R. H. Osborn, in *Cellulose and Cellulose Derivatives*, ed. by Emil Ott (Interscience Publishers, Inc., New York, 1943), p. 962 ff.

[5] W. Philippoff and K. Hess, Zeits. f. physik. Chemie **B31**, 237 (1936). K. Hess and W. Philippoff, Berichte **70**, 639 (1937).

[6] G. V. Schulz and F. Blaschke, J. prakt. Chemie **158**, 130 (1941).

[7] M. L. Huggins, J. Am. Chem. Soc. **64**, 2716 (1942).

[8] A. F. Martin, Abstract of Papers, Memphis Meeting of the American Chemical Society, April, 1942; cf. also reference 4.

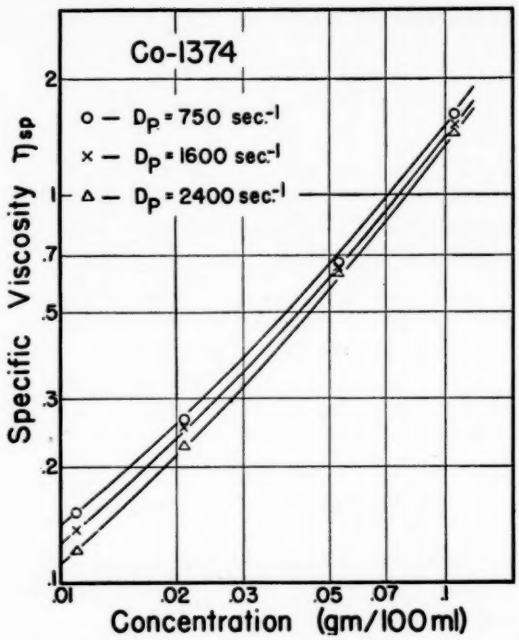

FIG. 2. Specific viscosity *vs.* concentration for cellulose Co-1374, in the range of low concentrations, showing the influence of velocity gradient.

k' and K are constants characteristic of solutes from a given homologous series in a given solvent.

While most, if not all of the various equations have at one time or another been considered in connection with the viscosity of solutions of high polymers, none of them explicitly recognizes the influence which velocity gradient has upon the viscous behavior of this class of solutions. Consequently, ambiguous results in the evaluation of η_i are obtained when data for the ranges of concentrations where the anomalous behavior has become appreciable, are substituted in the equations. Corresponding to each velocity gradient at which measurements are made there is (at any single concentration in the anomalous region) a different η_r or η_{sp}. Hence, as is evident from their form, equations of the type of (1), (2), and (3) will yield a different η_i for each velocity gradient. Conrad[2] has shown by numerical example that Eq. (1), written:

$$\eta_i = \frac{8}{c_0} = \frac{8}{c}(\sqrt[8]{\eta_r} - 1), \qquad (4)$$

and applied to data on 0.5 percent solutions of cellulose in cuprammonium, and on a 1 percent solution of nitrocellulose in Butyl acetate, yields intrinsic viscosities ranging from 8.67 to 16.67 in the first case, and from 6.70 to 28.24 in the latter, the particular value of the intrinsic viscosity depending on the mean gradient prevailing during measurement. Where equations which ignore the velocity gradient effect have been successfully applied to solutions in the higher range of concentration, it would appear that the constants are actually parameters associated with particular velocity gradients, or with certain sequences of velocity gradients during discharge, imposed by experimental conditions.

PROPOSED EQUATION FOR CONCENTRATION EFFECT

Because in ascertaining the exact concentration of a solution the error generally increases with dilution, it is often preferable to use concentrations sufficiently high that the anomalous behavior is still pronounced. It then becomes necessary, if one is to obtain reliable calculations of intrinsic viscosities, to have an equation for the concentration effect which recognizes the anomalous effect also. The remarkable success with which the Baker-Philippoff formula, Eq. (1), has been applied[5] to a large variety of high-polymeric solutions, over a wide range of concentrations, suggested that it could be profitably used as a basis for the required equation. Equation (1) is adjustable to different velocity gradients by virtue of the fact that c_0 takes a different value for each gradient. However, as appears from the foregoing remarks, and especially from Eq. (4), this implies

TABLE I. Relative viscosity η_r of cellulose in cuprammonium hydroxide at various concentrations c and velocity gradient D_P.

Sample	D_P (sec.$^{-1}$) / c (g/100 ml)	Zero	500	750	1660	2400
		Relative viscosities η_r				
Co-159	0.010	1.10*	1.11	1.11	1.10	1.10
	0.026	1.32*	1.25	1.25	1.25	1.23
	0.052	1.54*	1.52	1.52	1.52	1.51
	0.102	2.23*	2.23	2.22	2.15	2.23
	0.210	5.13*	4.69	4.57	3.89	3.78
	0.305	8.80*	7.69	7.33	6.40	—
	0.410	15.7*	12.5	11.6	—	—
	0.520	24.2*	19.6	18.0	—	—
Co-1374	0.011	—	1.14	1.15	1.14	1.12
	0.021	—	1.34	1.26	1.24	1.23
	0.053	—	1.72	1.67	1.66	1.63
	0.106	—	2.65	2.63	2.54	2.45
	0.215	—	5.54	5.40	4.93	4.59
	0.525	—	27.5	24.4	—	—

* Based on slopes at the origin of extrapolated D_P *vs.* τ_r curves.

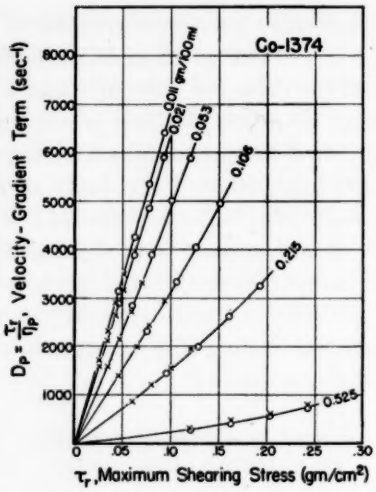

FIG. 3. Typical D_P *vs.* τ_r curves for cellulose in cuprammonium hydroxide.

that η_i is a function of velocity gradient. Evidently, if η_i as calculated is to be a material constant, the modified equation must contain a term whose evaluation is independent of velocity gradient, and must be of such form that the influence of the gradient disappears as $c \rightarrow$ zero.

If the right-hand side of Eq. (1) is expanded in a series we have:

$$\eta_r = \left(1+\frac{c}{c_0}\right)^8 = 1+8\frac{c}{c_0}+\frac{8\cdot 7}{2!}\left(\frac{c}{c_0}\right)^2 + \frac{8\cdot 7\cdot 6}{3!}\left(\frac{c}{c_0}\right)^3+\cdots, \quad (5)$$

$$\frac{\eta_r-1}{c} = 8\frac{1}{c_0}+\frac{8\cdot 7}{2!}\frac{c}{c_0^2}+\frac{8\cdot 7\cdot 6}{3!}\frac{c^2}{c_0^3}+\cdots. \quad (6)$$

Evidently, it is only the coefficient $8/c_0$ which remains when the $\lim_{c\rightarrow 0}$ is taken in Eq. (6). The fact that by definition this limit is the intrinsic viscosity η_i leads to the relation in Eq. (4). If we remove from the expression for η_r, Eq. (5), the term $8\,(c/c_0)$, and replace it with one involving a constant independent of velocity gradient, we shall obtain an analytical expression for the condition represented by Fig. 1, wherein the relative viscosity-concentration relation is independent of the velocity gradient as $c \rightarrow$ zero. This modification is achieved by writing

$$\eta_r = \left(1+\frac{c}{\lambda}\right)^8 + \left(k_i - \frac{8}{\lambda}\right)c, \quad (7)$$

where k_i is the new constant, and λ represents the parameter c_0 now interpreted as a function of velocity gradient. Here now,

$$\lim_{c\rightarrow 0}\frac{\eta_r-1}{c} = \eta_i = k_i \quad (8)$$

regardless of velocity gradient.

EXPERIMENTAL PROCEDURE

Viscosity determinations were made in accordance with the method already fully described by Conrad.[2] The capillaries used with the buret viscometers have a uniform length of 5.00 cm, and seven different bore radii ranging from 0.017 to 0.079 cm. Weighed samples of cotton cellulose were introduced into the burets in amounts calculated on the basis of moisture content to give concentrations near certain selected values. Exact concentrations, in g/100 ml of solution, were finally computed on the basis of cellulose content. The composition of the cuprammonium-hydroxide solvent was in accordance with the specifications of the Committee on the Viscosity of Cellulose of the American Chemical Society. Measurements of discharge times were made in a constant-temperature bath held at 25±0.05°C (extreme variation).

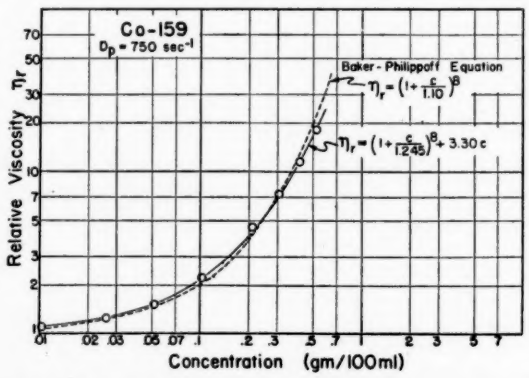

FIG. 4. Relative viscosity *vs.* concentration with $D_P = 750$ sec.$^{-1}$, showing curve of Eq. (7) with best-fitting Baker-Philippoff curve for comparison.

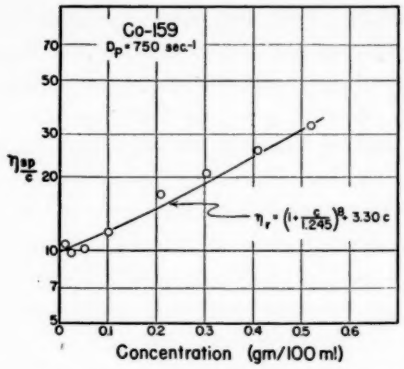

FIG. 5. Specific viscosity-concentration ratio *vs.* concentration; data of Fig. 4, with curve of Eq. (7).

MATERIALS

Two samples of cellulose were used. One of the samples, Co-159, obtained from Dr. R. E. Reeves of the staff of this Laboratory, had been prepared from a supply of Coker's Super-Seven cotton. It was extracted 8 hr. each with ethanol-benzene (in the ratio 1:1) and water. The extractions were followed by a treatment for 8 hr. at 75°C with a 1 percent solution of NaOH in an atmosphere of hydrogen. The second cellulose sample, Co-1374, was prepared from a carefully cleaned cotton by first thoroughly extracting the sample at a temperature held above 60°C, with 95 percent ethanol. After two washings with water, and drying in air, the sample was extracted for 8 hr. at the boiling point with a 1 percent NaOH solution. During this treatment purified nitrogen was bubbled through the cotton to keep any atmospheric oxygen swept out, and to provide agitation. The cotton was then washed free of alkali, immersed in 1 percent acetic acid, again thoroughly washed with distilled water, and finally dried. The cellulose content of the treated sample was found to be 94.7 percent of the air-dry weight.

For the purpose of calculating the relative viscosities, measurements of viscosity were obtained on the pure cuprammonium-hydroxide solvents. That used with sample Co-159 was found to have a viscosity of 0.01273 poise, while the solvent used with Co-1374 had a viscosity of 0.01293 poise, both values having standard errors within 0.36 percent.

TREATMENT OF DATA

From the flow-times and previously tabulated buret and capillary constants the fluidities of the cellulose solutions were calculated in accordance with the Poiseuille equation for each 5-ml section of the burets. Corrections for kinetic-energy losses were applied to the observed values, and the resulting apparent coefficients of viscosity η_P finally expressed in g-sec./cm^2. Using the mean hydrostatic head in each 5-ml section, as given by Meissner's formula, the shearing stress at the capillary wall τ_r was calculated by means of the equation

$$\tau_r = \frac{rP}{2l}, \qquad (9)$$

where r = capillary radius (cm), P = mean pressure (g/cm^2) converted from hydrostatic head, and l = length of capillary (cm). For the present study it was necessary to have a measure of the velocity gradient corresponding to each value of τ_r. For use with τ_r, the most reasonable choice is the velocity gradient D_P, which is given by the simple relation:*

$$D_P = \frac{\tau_r}{\eta_P}. \qquad (10)$$

The choice of this velocity gradient term as the representative velocity gradient is dictated solely by its relation to τ_r, for, as Eq. (10) shows, the ratio of the two gives the apparent, Poiseuille viscosity. For a Newtonian liquid D_P in Eq. (10) would be exactly the maximum velocity gradient, for here η_P is the "true" rather than "apparent" viscosity. The η_P has a uniform value throughout the cross section of the capillary, including the lamina adjacent to the wall. Thus, for a Newtonian liquid, D_P as given by

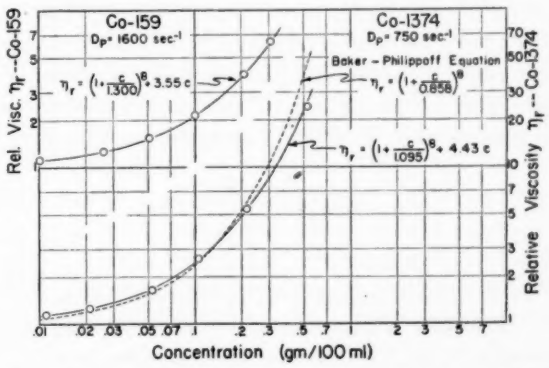
Co-159
D_P = 1600 sec.$^{-1}$
$\eta_r = \left(1 + \frac{c}{1.300}\right)^8 + 3.55c$
Co-1374
D_P = 750 sec.$^{-1}$
Baker – Philippoff Equation
$\eta_r = \left(1 + \frac{c}{0.858}\right)^8$
$\eta_r = \left(1 + \frac{c}{1.095}\right)^8 + 4.43c$
Rel. Visc. η_r --Co-159
Relative Viscosity η_r --Co-1374
Concentration (gm/100 ml)

FIG. 6. Relative viscosity *vs.* concentration for cellulose Co-159 with $D_P = 1600$ sec.$^{-1}$, and cellulose Co-1374 with $D_P = 750$ sec.$^{-1}$.

* Direct substitution of numerical values in the expression $(4V/\pi r^3 t) \equiv D_P$ would neglect kinetic-energy losses. The computation of D_P by Eq. (10) embraces the corrections for these losses.

Eq. (10), can be taken rigorously as the velocity gradient *at the wall*. While such studies as those of Kroepelin[9] permit us to conclude that, for anomalous liquids also, the maximum velocity gradient prevails at the capillary wall, this maximum value is not that given to D_P by Eq. (10). In anomalous liquids, the value of η_P as obtained by the present method is an average, or representative value for the whole cross section of flowing liquid, and is not exactly the viscosity in the lamina adjacent to the capillary wall, so that D_P is not the velocity gradient at this boundary. No rigorous analytical expression is yet available for the latter gradient, but its numerical value may be expected to be slightly greater than D_P.

RESULTS

From each series of observations at various selected concentrations, graphs of D_P *versus* τ_r, such as that shown in Fig. 3, were prepared. Each point represents a single observation of flow-time in a 5-ml section of the viscometer. Since the ratio of abscissa to ordinate on these graphs is η_P, the graphs were used for the interpolation of τ_r (and thence η_P) at the different concentrations for various chosen D_P's. To obtain rough estimates of η_P at zero velocity gradient ($D_P=0$), tangents to the curves were drawn at the origin, the inverse of the slopes of these tangents being the desired η_P.

In Fig. 4 are plotted the results* on one of the cellulose samples Co-159, for $D_P=750$ sec.$^{-1}$. The curve for Eq. (7) is drawn in, with $\lambda=1.245$ and $k_i-(8/\lambda)=3.30$, illustrating satisfactory agreement between Eq. (7) and experiment. The constants here give, in accordance with Eq. (8),

$$\eta_i=k_i=3.30+\frac{8}{1.245}=9.73.$$

On this graph is also drawn the best fitting curve of the Baker-Philippoff equation, c_0 having been evaluated by the method of averages, using the eight experimental points. This equation gives $\eta_i=(8/c_0)=7.27$. In Fig. 5 the same data are plotted as η_{sp}/c (on a logarithmic scale) *versus* concentration. The curve is for Eq. (7), using the same constants mentioned above. It will be seen to be slightly concave upward, rather than linear.

The relative viscosity of the same cellulose sample with $D_P=1600$ sec.$^{-1}$ is plotted in Fig. 6. The curve, representing Eq. (7), is drawn for $\lambda=1.300$ and $k_i-(8/\lambda)=3.55$. The corresponding value of η_i is 9.70, which is in satisfactory agreement with the value found above for the same cellulose at another gradient, $D_P=750$ sec.$^{-1}$. This agreement indicates the general applicability of Eq. (7) to various values of D_P, but cannot be taken as a proof of its validity.

Also plotted in Fig. 6 are the results on the other cellulose sample, Co-1374 for $D_P=750$ sec.$^{-1}$. Equation (7) adapted to these data yields for η_i the value $4.43+8/1.095=11.74$. The Baker-Philippoff curve tends to diverge from experiment toward excessively high values for η_r as concentration increases, a tendency found also in Martin's[4] graphs of this equation for a higher range of concentrations of cellulose in cuprammonium hydroxide.

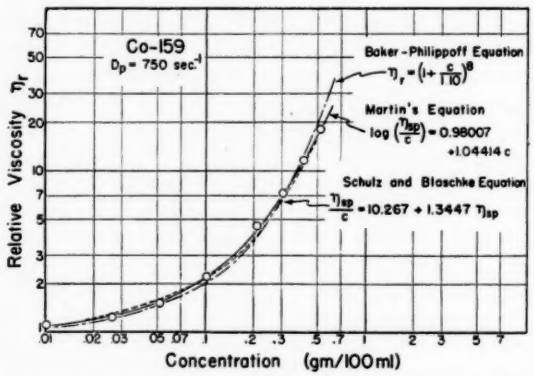

FIG. 7. Relative viscosity *vs.* concentration with $D_P=750$ sec.$^{-1}$, showing best-fitting curves calculated according to the Baker-Philippoff, the Schulz and Blaschke, and the Martin equations.

DISCUSSION

The results of the present investigation indicate that in addition to being in satisfactory agreement with experimental data, Eq. (7) is of such form as to yield a uniform value for the intrinsic viscosity η_i for various velocity gradients. The latter property evidently has required the introduction of two constants into the em-

[9] H. Kroepelin, J. Rheology **2**, 385 (1931).

* In the results reported in this paper, $\eta_r=\eta_P/\eta_0$, where η_0 is the viscosity of the solvent.

pirical equation, while only one c_0 appears in the original Baker-Philippoff equation. It is significant that two constants also appear in Eqs. (2) and (3), and that these equations, as Fig. 7 indicates, are in good agreement with experiment. Thus, it might be inferred that two constants are required in equations relating viscosity and concentration, especially in view of the failure (when applied to high-polymer solutions) of the older equations involving only one constant. Since solutions of the long-chain polymers generally exhibit anomalous viscous behavior, the necessity for two constants might be rationalized on the theory that one constant represents an enduring property of the solute-solvent system, reflected by the intrinsic viscosity, while the other constant represents the conditions of flow, as reflected by velocity gradient. In Eq. (7) these two factors are recognized; k_i is identified as the intrinsic viscosity η_i, while λ is introduced as a function of velocity gradient D_P as well as of η_i. In both Eqs. (2) and (3), η_i appears as one of the two constants. The other two constants k' and K, however, have not up to the present been interpreted as terms reflecting flow conditions. As presently interpreted, k' and K are constants for a given solute-solvent system, and are not means for compensating for differences in the velocity gradients at which viscosities may be measured. Hence if η_{sp} is computed from readings taken in the anomalous region, the Schulz and Blaschke and the Martin equations, like the Baker-Philippoff equation, will evidently yield different values for η_i, depending on the prevailing velocity gradient. Whether k' and K are actually insensitive to differences in velocity gradient would appear to be a suitable subject for further study. In this connection, it may be remarked that Martin's equation, with constants evaluated from the present data, and represented by the curve in Fig. 7, has $K=0.109$ while Martin[8] himself gives the value of 0.130 for cellulose in cuprammonium hydroxide. A difference in velocity gradient suggests itself as a possible reason for the difference in the value of K.

TABLE II. Intrinsic viscosity η_i of cellulose in cuprammonium hydroxide, sample Co-159, as calculated according to two equations at two different velocity gradients D_P.

	$D_P=750$ sec.$^{-1}$	$D_P=1600$ sec.$^{-1}$
Baker-Philippoff, Eq. (1)	7.42, 8.23 / Mean 7.82	6.74, 7.84 / Mean 7.29
Eq. (7)	9.29	9.33

A means of comparing the equations under discussion here is afforded by the values of η_i given by each. The following values of η_i are those corresponding to the data plotted in Figs. 4 and 7:

Baker-Philippoff, Eq. (1)	7.27
Schulz and Blaschke, Eq. (2)	10.27
Martin, Eq. (3)	9.55
Eq. (7)	9.73.

It will be noted that the two latter equations, which give values of η_i in fair agreement with each other, are also the two which yield curves best fitting experimental points in Fig. 7. Such agreement between empirical equations of dissimilar form, as to a value which is essentially an extrapolation, tends to enhance the reliability of either of the two values of η_i.

The above-recorded values of η_i are based on observations at eight different concentrations, this number being employed in the present study to test and compare the various equations. An acceptable formula, however, should yield a reliable value for η_i for a given sample with much fewer observations. From what has been said regarding the character of the parameters λ and k_i in Eq. (7), it is evident that neither one can be fixed by the *type* of macromolecule in solution. Also the comparison of the values of λ in Figs. 4 and 6, for the two different cellulose samples, *viz.*, 1.245 and 1.095, both for $D_P=750$ sec.$^{-1}$, indicates quite clearly that λ does not remain constant with D_P. It thus appears that two unknowns, λ and k_i, must be evaluated for each sample. Hence viscosity determinations at two concentrations, adjusted to a common D_P (or a common *mean* velocity gradient), are necessary and sufficient to evaluate η_i according to Eq. (7). In Table II intrinsic viscosities obtained with this equation at two velocity gradients are compared with those obtained with Eq. (1) using the same original data. These data are those plotted in Figs. 4 and 6 for Co-159 at $c \leqq 0.10$ and 0.30 g/100 ml. While the value of η_i given by Eq. (1) varies over a range of 20 percent of the mean, that given by Eq. (7) has a range of 0.4 percent.

That the value of η_i given by this equation in Table II is lower than the value 9.73 recorded above evidently arises from the fact that the observations at $c \leqq 0.30$ g/100 ml are slightly out of line. The data at this concentration greatly influence the results in Table II, where only two concentrations are involved. The equations cannot improve on the observations, and must reflect discrepancies in the latter.

THEORETICAL CONSIDERATIONS

With the present limited knowledge of the intermolecular processes occurring during viscous flow in high-polymer solutions, there is little theoretical basis for attempting a choice between Eqs. (2), (3), and (7). Schulz and Blaschke's equation written

$$\eta_r = 1+\eta_i c+k'(\eta_i c)^2+k'^2(\eta_i c)^3+\cdots, \quad (11)$$

Martin's equation written

$$\eta_r = 1+\eta_i c+2.30K(\eta_i c)^2 + \frac{(2.30K)^2}{2!}(\eta_i c)^3+\cdots, \quad (12)$$

and Eq. (7) written

$$\eta_r = 1+\eta_i c+\frac{8\cdot 7}{2!}\left(\frac{c}{\lambda}\right)^2+\frac{8\cdot 7\cdot 6}{3!}\left(\frac{c}{\lambda}\right)^3+\cdots, \quad (13)$$

show remarkable similarily. Each of these equations, evidently, is effectively an empirical revision of the Einstein equation $\eta_r = 1+\eta_i c$, the differences being in the coefficients of the higher powers of c which are introduced to account for the experimental consequences of complicated intermolecular forces and conditions peculiar to solutions of long-chain polymers. Each of the expansions involve η_i as well as another parameter; the absence of η_i from the higher power terms of Eq. (13) is only apparent, for λ is evidently a function of η_i.

The Eyring[10] reaction-rate theory of viscosity provides a possible theoretical basis for Eqs. (11)—(13), though it does not lend support to any particular one. The fundamental equation in this theory is:

$$\eta = \frac{fs_1}{s\left[\exp\left(\frac{fs_2s_3s}{2kT}\right)-\exp\left(\frac{-fs_2s_3s}{2kT}\right)\right]}\frac{h}{kT} \cdot \frac{F_n}{F_a^*}\exp\left(\frac{\Delta E_a}{kT}\right), \quad (14)$$

where η = coefficient of viscosity; f = force per cm² tending to displace one molecular layer with respect to another; s = distance between equilibrium positions in the direction of flow; s_1 = perpendicular distance between adjacent layers of molecules; s_2 = distance between adjacent molecules in direction of flow; s_3 = distance between molecules in the plane of flow and normal to the direction of flow; F_n, F_a^* = partition functions; $\Delta E_a \doteq$ energy of activation; h = Planck's constant; and k = Boltzmann's constant. Now,

$$\exp\left(\frac{fs_2s_3s}{2kT}\right)-\exp\left(-\frac{fs_2s_3s}{2kT}\right)=2\sinh\frac{fs_2s_3s}{2kT}.$$

For the present experiments on cotton cellulose in cuprammonium hydroxide, let us assume

$$1\text{A} < s_2 \leqq s_3 < 5\text{A}, \quad \text{and} \quad s < 10\text{A},$$

so that $s_2s_3s < 250\text{A}^3$. The maximum shearing stress $\tau_r \leqq 0.25$ g/cm². Hence $f < 245$ dynes/cm², and

$$fs_2s_3s < 6.1\cdot 10^{-22} \text{ erg.}$$

At 25°C,

$$2kT = 8.2\cdot 10^{-14} \text{ erg.}$$

Hence, we may say: $fs_2s_3s \ll 2kT$, and under this condition,

$$2\sinh\frac{fs_2s_3s}{2kT} \leqq 2\left(\frac{fs_2s_3s}{2kT}\right).$$

Equation (14) becomes then,

$$\eta = \frac{fs_1}{s\dfrac{fs_2s_3s}{kT}}\cdot\frac{h}{kT}\cdot\frac{F_n}{F_a^*}\exp\left(\frac{\Delta E_a}{kT}\right) = \frac{s_1h}{s_2s_3s^2}\cdot\frac{F_n}{F_a^*}\exp\left(\frac{\Delta E_a}{kT}\right). \quad (15)$$

[10] H. Eyring, J. Chem. Phys. **4**, 283 (1936). R. H. Ewell, J. App. Phys. **9**, 252 (1938), especially p. 254.

Kauzmann and Eyring[11] have shown that the energy of activation ΔE_a for viscosity in normal paraffins increases with the chain length. This would seem to be in accord with the interpretation of activation energy given by Ewell,[10] as the work required to provide space into which a molecule can flow. Evidently, more energy will be required to dislodge a single macromolecule with many points of attraction than would be required to produce shifts in the positions of an equal volume of smaller uncombined molecules. The introduction of chain molecules into a solvent liquid, then, will tend to increase the average activation energy, and for dilute solutions this increment may be supposed to be directly proportional to the number of high-polymer solute molecules in unit volume, i.e., the concentration c. Thus, the activation energy for viscous flow in a dilute, high-polymer solution is $\Delta E_{a,0}+Bc$, $\Delta E_{a,0}$ being the activation energy for the pure solvent. The proportionality factor B may be supposed to be a function of the velocity gradients prevailing between the various shearing layers, if, as seems likely, the orientation of the chain molecules influences their activation energies. The effect of the long-chain structure is offset by a high degree of orientation, which in turn, is associated with a high velocity gradient. We may, therefore, expect B to decrease with increasing velocity gradient, though not necessarily in a linear relationship.

For a high-polymer solution, then,

$$\eta=\frac{s_1 h}{s_2 s_3 s^2}\cdot\frac{F_n}{F_a^*}\exp\left(\frac{\Delta E_a+Bc}{kT}\right),$$

$$=\eta_0\exp\frac{Bc}{kT}. \qquad (16)$$

For constant temperature and velocity gradient, this equation becomes

$$\ln\frac{\eta}{\eta_0}=\ln\eta_r=\text{constant}\cdot c, \qquad (17)$$

which is Arrhenius' formula for the concentration effect.

Expanding Eq. (16), we have

$$\eta_r=\frac{\eta}{\eta_0}=1+\left(\frac{B}{kT}\right)c+\frac{1}{2!}\left(\frac{B}{kT}\right)^2 c^2+\frac{1}{3!}\left(\frac{B}{kT}\right)^3 c^3+\cdots. \qquad (18)$$

In this equation the reaction-rate theory of viscosity evidently supplies a better theoretical basis than does the Einstein formula, for the many serially-expandable, empirical equations, such as Eqs. (11)–(13), expressing the concentration effect. While the Einstein treatment provides no interpretation of the higher powers of c which appear in the empirical equations, these powers seem to be a natural consequence of the Eyring theory.

Equation (18) is not completely in accord with the empirical equations, excepting, of course, the Arrhenius equation. There are evidently second-order effects which the derivation of Eq. (18) has neglected. However, the comparison of this equation with Eqs. (11)–(13) reveals a close relationship, if not identification, between B/kT and η_i. The implied dependence of η_i on B, and hence on velocity gradient, is unsatisfactory, and inconsistent with the current interpretation of η_i as an absolute, material constant. On the other hand, the appearance of B in the expression B/kT in Eq. (18) indicates that the coefficients of the higher powers of c should be functions of not only temperature, but also velocity gradient. The dependence on the latter factor was found in the present experiments (for all of which T=constant), and is reflected in the appearance of λ in the coefficients of Eq. (13). As indicated previously, B, and therefore the coefficients, should be expected to decrease with increasing gradient. The present results confirm this theory; thus, for $D_P=750$ sec.$^{-1}$, $\lambda=1.245$, while for $D_P=1600$ sec.$^{-1}$, $\lambda=1.300$, in sample Co-159. Equations (11) and (12) make no explicit provision in the coefficients for the influence of velocity gradient, though Huggins, in his theoretical deduction of Eq. (2), interprets k' as a kind of shape factor. Since the shape of the chain molecules may conceivably depend on velocity gradient, there is the suggestion that gradient may influence the value of the coefficients in Eq. (11).

[11] W. Kauzmann and H. Eyring, J. Am. Chem. Soc. **62**, 3113 (1940).

SUMMARY

The present study calls attention to the fact that the viscosity-concentration relationship for a high-polymer solution such as that of cellulose in cuprammonium hydroxide depends on the velocity gradient at which the viscosity is measured. This dependence is reflected by changes in the values of the parameters in the expression for the viscosity-concentration effect given by Eq. (7). In such formulas as the Baker-Philippoff equation the alteration of the values of the so-called constants alters the computed η_i, while with Eq. (7), and probably other equations employing more than one parameter, the substitution of data for different velocity gradients yields a substantially uniform value of η_i. Equation (7) is of most interest as an example of the type of equation required for the viscosity-concentration effect; the evaluation of λ and k_i being quite tedious, the equation does not recommend itself for easy application. The partial conformity which has been pointed out between the expanded expression for η_r in Eq. (13) and Eq. (18), based on the reaction-rate theory of viscosity, would appear to lend support to a relation of the type of Eq. (7).

ACKNOWLEDGMENTS

The experimental observations in this investigation, and the preliminary computations on the data, were made with much care by Verne W. Tripp. To Dr. Carl M. Conrad, in general charge of cotton-cellulose fluidity investigations in this Laboratory, the writer is indebted for his helpful interest and stimulating discussions on issues raised in the foregoing study.